Spring 2013

NIR light transmission through skin and muscle

Deniz Ozgulbas
New Jersey Institute of Technology

Copyright Warning & Restrictions

The copyright law of the United States (Title 17, United States Code) governs the making of photocopies or other reproductions of copyrighted material.

Under certain conditions specified in the law, libraries and archives are authorized to furnish a photocopy or other reproduction. One of these specified conditions is that the photocopy or reproduction is not to be "used for any purpose other than private study, scholarship, or research." If a, user makes a request for, or later uses, a photocopy or reproduction for purposes in excess of "fair use" that user may be liable for copyright infringement,

This institution reserves the right to refuse to accept a copying order if, in its judgment, fulfillment of the order would involve violation of copyright law.

Please Note: The author retains the copyright while the New Jersey Institute of Technology reserves the right to distribute this thesis or dissertation

Printing note: If you do not wish to print this page, then select "Pages from: first page # to: last page #" on the print dialog screen

ABSTRACT

NIR LIGHT TRANSMISSION THROUGH SKIN AND MUSCLE

by
Deniz Ozgulbas

Light has been used extensively in the medical field for both therapeutic and diagnostic applications. Tissue optical window or therapeutic window defines the range of wavelengths where the light has the maximum transmittance through tissue. In this range, absorption and scattering effects are relatively lower when compared to the visible or middle infrared wavelengths. Knowledge of the transmittance through tissue can help determine the effective light intensities in medical applications.

The objective of this thesis is to determine the NIR light transmission through different thicknesses of animal tissue and its spatial spread due to the scattering effect. Primarily pork skin and muscle tissues are used due to their similar optical properties to human tissue. Tissue thicknesses range from 4 mm to 20 mm. A NIR LED array with the wavelength of 875 nm serves as the light source. A commercial photodiode is used for measurements of the transmitted light intensities.

The results demonstrate a transmittance of 18% for 4 mm tissue thickness and 3% for 20 mm and vary exponentially in between. Scattering increases the spatial spread of the light beam and makes it very difficult to focus inside the tissue. In addition to the transmittance measurements, temperature elevation due to the NIR light illumination is investigated. Thermocouple measurements show a temperature increase of 1.2 ^{o}C on the surface of the tissue slab at the light intensities tested in this project.

NIR LIGHT TRANSMISSION THROUGH SKIN AND MUSCLE

by
Deniz Ozgulbas

A Thesis
Submitted to the Faculty of
New Jersey Institute of Technology
in Partial Fulfillment of the Requirements for the Degree of
Master of Science in Biomedical Engineering

Department of Biomedical Engineering

May 2013

APPROVAL PAGE

NIR LIGHT TRANSMISSION THROUGH SKIN AND MUSCLE

Deniz Ozgulbas

Dr. Mesut Sahin, Thesis Advisor Associate Professor of Biomedical Engineering, NJIT	Date
Dr. Tara Alvarez, Committee Member Associate Professor of Biomedical Engineering, NJIT	Date
Dr. Raquel Perez Castillejos, Committee Member Assistant Professor of Biomedical Engineering, NJIT	Date

BIOGRAPHICAL SKETCH

Author: Deniz Ozgulbas

Degree: Master of Science

Date: May 2013

Undergraduate and Graduate Education:

- Master of Science in Biomedical Engineering,
  New Jersey Institute of Technology, Newark, NJ, 2013

- Bachelor of Science in Electronics Engineering,
  Ankara University, Ankara, Turkey, 2011

I would like to dedicate this work to my family, my dear wife and my lovely niece.

ACKNOWLEDGMENT

I am grateful to my thesis advisor, Dr. Mesut Sahin for providing guidance, enthusiasm and support throughout this project. I would like to thank Dr. Raquel Perez Castillejos and Dr. Tara L. Alvarez for participating in my committee and providing feedback. I would like to thank John S Hoinowski for his help and advice for the experimental setup. I am thankful to Atabek Can Yucel for his help in the Pro-E drawings. Thanks also go to my dear friend Eren Alay and Neural Interface Laboratory members for their support.

I would like to thank my beloved family and my wife for their continuous support and encouragement.

TABLE OF CONTENTS

TABLE OF CONTENTS
(Continued)

Chapter **Page**

LIST OF TABLES

LIST OF FIGURES

LIST OF FIGURES
(Continued)

LIST OF FIGURES
(Continued)

Figure **Page**

CHAPTER 1

INTRODUCTION

1.1 Objective

Developments in the medical field have introduced new technologies for bidirectional information transfer between body and external devices. Percutaneous wires are widely used due to large bandwidth and low power requirements for transferring information. However, percutaneous connectors are in general not well tolerated by the body for long term. Moreover, wires induce infection, mechanical stress and pain [1].

The problems related with the wired electrodes can be resolved by wireless methods. Telemetry methods are emerging to record signals, activate devices, or stimulate nerves transcutaneously in the medical field. RF power telemetry, optical and acoustic telemetry are commonly used to activate implanted microstimulators. RF methods can provide high speed communication, and do not introduce any harmful and residual effects to the body [2]. On the other hand high level energy requirements, the bulky extracorporeal equipment, and the susceptibility to electromagnetic noise coming from the external devices are the disadvantages of RF telemetry [1, 3]. Acoustic methods are also susceptible to environmental acoustic noise, requires high power, and additional equipment [1].

Optical telemetry is an alternative solution for the methods listed above for transferring information between the implanted and the external device. Optical telemetry methods are non-invasive, compacter than other methods, and have less susceptibility to noise. Most biological tissues have relatively low light absorption

property in the NIR spectral region. Transmittance through tissues is an important factor in optical telemetry system designs.

The objective in this thesis was to determine the light penetration parameters such as the depth of penetration and spatial spread at NIR wavelengths through skin and muscle tissue. In addition, the temperature rise at the surface of the tissues due to NIR beam was investigated.

1.2 Medical Applications of Light

Light has been widely used in medical applications. Optical radiation used in medical field is generally safe except UV radiation [4]. Moreover, optical methods are generally non-invasive, cost effective, and insensitive to electromagnetic interference [5].

Light has been used in medicine since ancient times. The Ancient Greeks in Heliopolis (i.e. the Greek city of sun), broke up the sunlight into its spectral components to treat specific medical problems [6]. Most of the light spectrum is being used by medical applications recently. Optical radiation wavelengths range from 1nm to 1mm. This region starts from the soft ionizing X-Ray domain to the infrared domain. Optical radiation has photochemical (i.e. UV), thermal (IR) or both (visible range) effects [7]

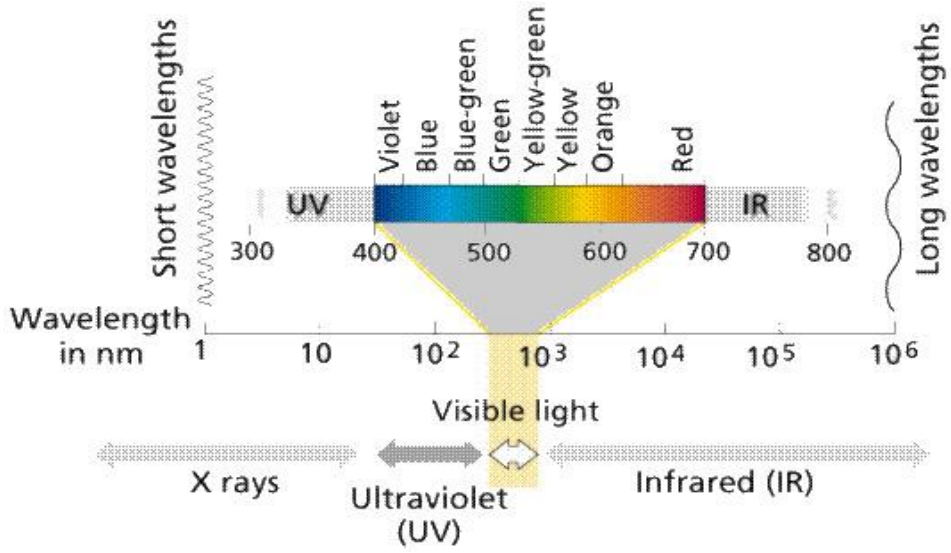

Figure 1.1 The electromagnetic light spectrum.

Source: http://www.emc.maricopa.edu/faculty/farabee/biobk/spectrum.gif, (accessed March 28 2013)

The use of light in medicine has advanced with the emerging technology, in particular development of the LASER's, LED's, optical fibers and optical detectors. The word LASER stands for **L**ight **A**mplification by **S**timulated **E**mission of **R**adiation. Lasers emit highly directional high intensity beams which have precise wavelengths with narrow bandwidths [8]. LED is the acronym of Light Emitting Diode. LEDs are semi-conductor devices that emit light over broad range of wavelengths with wider bandwidths than LASER's.

This chapter will discuss some of the optical methods briefly to provide general information for those applications and their usage.

1.2.1 Low Level Light Therapy

Low Level Light Therapy (LLLT), also known as photobiomodulation is being used in medical field popularly. LLLT is being used in neurorehabilitation, and therapeutic applications such as wound healing, reducing pain, inflammation and, swelling [9] after the invention of the lasers and LEDs. LLLT uses low light powers in the range of

1-1000 mW, and the wavelength changes from 632-1064 nm to induce biological response in the tissues [10]. LLLT is also called as “cold light” therapy since the applied light power does not heat the tissues [9]. LLLT initially used coherent laser light as a light source, however after the development of NASA LEDs, they are now generally used in LLLT [11]. Also LEDs are cheaper and less dangerous solution than lasers. At a high level, LLLT works by triggering a photochemical reaction in the cell; when light interacts with certain molecules named chromophores [10]. Respective sections will discuss some of the applications of LLLT in the medical field.

1.2.2 Wound Healing

One of the first applications of LLLT was wound healing. In 1967, Helium neon (HeNe) lasers were used by Mester et al to treat patients with skin ulcers [10]. It is believed that LLLT is able to affect the three phases of wound healing: the inflammatory phase, proliferative phase and the remodeling phase [9]. Although the underlying mechanism of how LLLT promotes wound healing is not known exactly, it is believed that LLLT triggers the local release of cytokines, chemokines, and other biological mechanisms which decrease the wound closure time, and increase the breaking strength of the wound [9].

The results of the clinical studies are conflicting. For instance, Kana et al. used HeNe laser (wavelength, 632.8 nm) and argon laser (wavelength, 514.5 nm) at a constant power density of 45 mW/cm^2 to determine the effect of laser light on open skin wounds in rats [12]. They demonstrated that the laser treatment decreases the time required for wound closure. However, Anneroth et al. and colleagues investigated the effect of low energy infrared laser treatment on wound healing of rats [13]. Rats were wounded in their back area bilaterally and one side was treated with laser and the other side was left untreated as a control. The researchers observed that

the wound healing process was same for both laser treated and untreated wounds [13]. Similarly human studies were also showed conflicting results. Schindl et al. claimed that the application of HeNe laser promoted wound healing in 3 patients, on the other hand, Lundeberg et al. didn't observe a statistically significant difference between leg ulcer patients who were treated with HeNe laser and the placebo group [9].

Although, lasers are widely used clinically, they have some inherit characteristics that create problems in wound healing treatment. For instance, large wounds cannot be treated effectively with lasers due to their narrow beam width. Moreover, the lasers are limited on the wavelength selection which limits application of various wavelengths to the wounded area [11]. Furthermore, since the lasers produce highly collimated lights, they can induce heat production in tissue and the laser light can damage the eye. Due to these reasons, researchers are currently testing LEDs as an alternative solution to the lasers.

Contrary to lasers, LEDs can be configured to produce multiple wavelengths, they can be organized in large arrays to treat large area wounds, and they do not produce as much heat [11]. With the development of the NASA LEDs for medical care of astronauts, wound healing treatment showed great promise. Basically, NASA LEDs triggers the basic energy processes in the mitochondria of each cell, to activate the color sensitive chemicals (chromophores, cytochrome systems) [14].

U.S Navy researchers probed the effectiveness of LED light therapy on lacerations in submarine crew members. Since the submarine environment has low oxygen, high carbon dioxide, and lacks sunlight; thus the healing of the wounds in this environment takes longer than the surface. The reports demonstrated a 50% faster healing of lacerations in crew members that received LED treatment with three

wavelengths (combined in a single unit with wavelengths of 670, 720, 880 nm) compared to untreated control healing [11].

Although LLLT is generally used to cure wide range of diseases, there aren't enough clinical studies to prove or disprove its efficacy in wound healing for two reasons. First, the light parameters such as pulse properties, wavelength, power, and the timing should be adjusted for each treatment. Secondly, the underlying mechanism of how LLLT promotes wound healing has not been understood clearly [9]. Further investigations will provide better understanding of the mechanism of LLLT, and will give optimal light parameters for the therapies.

1.2.3 Neurorehabilitation

1.2.3.1 Stroke

LLLT application in medical field is not limited to wound healing. Recently, LLLT is being used for treatment of serious neurological conditions such as traumatic brain injury, stroke, spinal cord injury, and degenerative central nervous system disease [9]. For stroke treatment, Oron et al and colleagues investigated the effect of transcranial LLLT on stroke induced rats [15]. They induced stroke by two different ways (1) permanent occlusion of the middle cerebral artery through a craniotomy or (2) insertion of a filament. In the post stroke term, rats were treated transcranially with a Ga-As laser diode to illuminate the hemisphere contralateral to the stroke. Results showed that noninvasive application of LLLT 24 hours after the induction of stroke was significantly improved the neurological function of rats [15].

Moreover, transcranial LLLT also showed promising results in acute human stroke patients. Lampl Y. et al and colleagues used an NIR (808 nm) laser with a power density of 7.5 mW/cm^2 to evaluate the ability to improve the outcomes of

human ischemic stroke [16]. They applied the laser to the entire surface of the head regardless of the stroke location after 18 hours of the stroke onset and the patients showed significant improvements [16]. Lampl et al [16] wrote that "Although the mechanism of action of infrared laser therapy for stroke is not completely undertood… infrared laser therapy is a physical process that can produce biochemical changes at the tissue level. The putative mechanism… involves stimulation of ATP formation by mitochondria and may also involve prevention of apoptosis in the ischemic penumbra and enhancement of neurorecovery mechanisms."

1.2.3.2 Traumatic Brain Injury

In the United States, annually, more than 1.4 million new cases of TBI occur, and more than 80,000 persons are left with permanent disability [10]. Traumatic brain injury (TBI) is a severe health problem and the therapies for this problem have not been successful enough. Recently, LLLT is also being investigated as an alternative method for traumatic brain injury treatment to the previous methods. Experiments on rats showed that LLLT could decrease the brain damaged area at 3 days following treatment, and specifically treatment with a 665 nm and 810 nm laser could yield to a statistically significant difference in the Neurological Severity Score (NSS) of mice which was injured by a weight being dropped onto the exposed skull [17].

In humans, two people with chronic mild TBI received a series of treatments with transcranial, red (693 nm), and NIR LEDs (870 nm) [18]. The LED cluster heads were applied to the patient's frontal, parietal, and temporal areas bilaterally. The results showed that both patients improved cognition after the treatment [18]. It is believed that LLLT inhibits apoptosis, stimulates angiogenesis, and increases neurogenesis in TBI treatment [9, 10].

So far, none of the LLLT studies have reported an adverse effect. LLLT will be more effective in the medical treatments with the help of developing technology and clinical studies.

1.2.4 Transcutaneous optical telemetry systems

In the past few decades, medical device area grew rapidly. Implantable medical devices could be one example of the medical device area developments. For example, cardiac pacemakers, defibrillators, cochlear prosthesis, bladder stimulators, and generic communication systems are some of the examples of implantable medical devices [19, 20]. Currently, most of the implantable devices especially cortical interfacing systems (e.g., Brain Gate System, Cyberkinetics Neurotechnology Inc.) are using percutaneous connectors, RF, and ultrasound to communicate between the implanted device and external control systems [21]. All of these methods have pros and cons.

Percutaneous wires have a larger bandwidth and low power consumption on the other hand usage of fine wires create mechanical stress as the patient moves and results in breakage and tissue infections [22]. Also, when the wires are broken, the communication path between the implanted device and external controller is damaged, thus the implanted device will be useless eventually and another surgical operation is required to implant the device again. Moreover, the wires are prone to electromagnetic interference from the environment.

RF is a well-established technology in implantable devices. Although RF methods can provide high speed communication; the high power consumption, interference from other sources, and limited bandwidth are the major problems of this method [21].

Optical transcutaneous link provides contact free communication with high data rates and electromagnetic noise immunity [23]. The main challenge of using transcutaneous optical telemetry is the light transmission through skin and tissue. While the light photons are transmitting through the skin and tissue, they are being scattered and absorbed by the surrounding tissue. The light tissue interaction will be discussed in the next chapter in detail.

A low powered and high data rate wireless optical link for implantable data transmission was proposed by Liu et al. [21]. They used a VCSEL with 850 nm wavelength, and operated the VCSEL with an on-off keying technique and a custom designed low power VCSEL driver to transfer data at 50 Mbps through 4 mm pork tissue, with a tolerance of 2 mm misalignment and a BER of less than 10^{-5}. Additionally, the power consumption of the system was 4.1 mW or less [21].

Similarly, Goto et al. investigated an optical telemetry system which consisted of a small implantable transmitter, external receiver, and chicken tissue [24]. The transmitter consisted of a near infrared LED (735 nm), to send a signal to the receiver, and six photodiodes to generate carrier wave, and power when they are transcutaneously irradiated. They successfully achieved optical data transmission through 7 mm thick chicken tissue, with the irradiation intensity range of 3.2-19 mW/cm^2 [24].

Okamoto et al. developed a bidirectional transcutaneous optical data transmission system using amplitude shift keying (ASK) modulation to monitor and control an artificial heart [25]. The system had two narrow directional LEDs; 590 nm visible LED was used to send data from outside of the body to the inside of body, on the other hand 940 nm infrared LED was used to send data in the opposite direction. Additionally, ASK modulator generated a carrier pulse signal (50 kHz) to achieve

maximum data transmission rate of 9600 bps. The in vitro experiments demonstrated that optical communication was achieved without error, with a tissue thickness of 45 mm for infrared light and 20 mm for visible light. The electric power consumption of the system was 122 mW for near infrared light and 162 mW for visible light [25].

Moreover, optical telemetry is also being used to activate the implanted neural stimulation devices in the central nervous system. Abdo et al. proposed a floating light activated microelectrical stimulator (FLAMES) to activate neural tissue using near infrared light [22]. The FLAMES contains silicon PIN photodiodes that are activated by the use of near infrared light through neural tissue. They implanted the FLAMES in rat spinal cord, and applied NIR pulses (0.2 ms, 50 Hz, 830 nm) to activate the device wirelessly, thus stimulate the spinal cord. As a result, ipsilateral forelimb movement, due to the intraspinal stimulation was observed. They measured the largest force around 1.08 N which was a significant level of force for the rat forelimb motor function [22].

In conclusion, optical telemetry is potential method to transfer information transcutaneously to several implanted devices. Optical telemetry systems do not require wires, less prone to noise compared to the other methods, have large bandwidths, and require less power. As the device technology continues to advance, more efficient optical techniques will be introduced to medical field.

1.2.5 Optical Nerve Stimulation

For a long period of time electrical methods have been used to stimulate neural activity, and it is still considered for new applications. Electrical methods are controllable, quantifiable, reliable, and spatially selective when compared to the chemical, mechanical, or magnetic stimulation methods [26]. Although electrode

designs and stimulation approaches have been advanced greatly, there are still limitations associated with electrical neural stimulation. Limitations of the electrical stimulation can be listed as; (1) tissue- electrode interface related problems such as toxicity of electrode material, tissue impedance and coupling, (2) stimulation artifact [26], (3) poor spatial selectivity [27]. To eliminate the limitations, researchers have sought new ways for neural stimulation.

In 2005, Wells et al. published a novel method, in which the neural stimulation of rat sciatic nerve was achieved optically by using low level, pulsed infrared laser without a damaging the tissue [27]. Moreover, as a result of optical stimulation of the rat sciatic nerve and muscle potentials showed similar responses to the conventional electrical neural stimulation [27, 28]. They defined the optical stimulation or infrared nerve stimulation as "The direct induction of an evoked physiological potential in response to a transient targeted deposition of optical energy. This implies that only a pulsed source can be used for stimulation of neural tissue." [29]. Soon after the discovery of this novel method, researchers at Northwestern University probed the possibility of optical stimulation of cochlear neurons. Izzo et al. used a pulsed laser diode (1.94 μm) at 2 Hz the radiant exposures ranged from 50 mJ/cm^2 to stimulate auditory neurons of the gerbil [30]. They evoked compound action potentials with the laser pulses and successfully stimulated the gerbil auditory neurons.

The novel optical nerve stimulation method can stimulate the neurons using low intensity, pulsed infrared light with the advantage of spatial selectivity, contact and artifact free stimulation [31]. Based on the promising results from animal studies, it is anticipated that the optical nerve stimulation will lead to clinical trials. Furthermore, the better understanding of biophysical mechanisms of optical stimulation will yield to new innovations in this area.

CHAPTER 2

FUNDAMENTALS OF TISSUE OPTICS

The application of light in medical field is growing rapidly. The optical properties of target tissues are important to develop effective devices and methods. Light propagation in biological tissue characterized by basic optical properties; absorption, scattering, and refractive index.

2.1 Refractive Index

Refractive index or index of refraction defines the light propagation speed in the medium. Refractive index is defined as;

$$n = \frac{c}{v} \tag{2.1}$$

where, c is the speed of light in vacuum, and v is the speed of light in the substance. Refractive index changes, it could be either continuous or sudden changes at boundaries, yield to scattering, refraction and reflection.

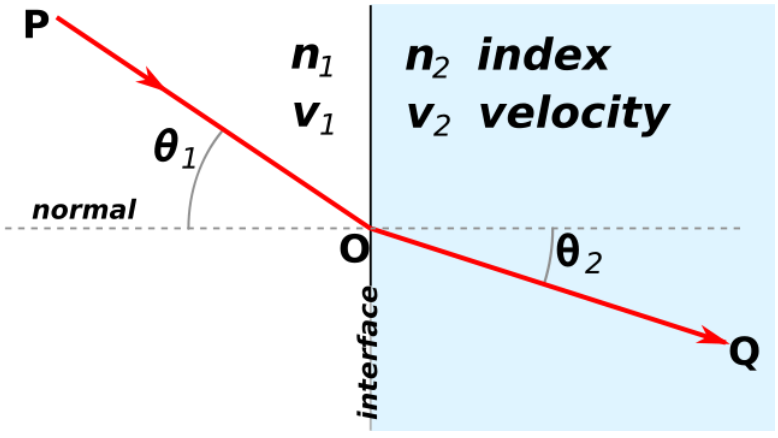

Figure 2.1. Refraction of light at the interface between two media of different refractive indices.

Source: https://upload.wikimedia.org/wikipedia/commons/thumb/d/d1/Snells_law.svg/641px-Snells_law.svg.png, (accessed March 28 2013).

Refraction occurs when the light enters a medium that has a different indice of refraction. Refraction of light is described by Snell's law;

$$\frac{sin(\theta_1)}{sin(\theta_2)} = \frac{v_1}{v_2} = \frac{n_2}{n_1} \tag{2.2}$$

Where, θ_1 is the angle of incidence, θ_2 is the angle of refraction; v_1 and v_2 are the speeds of light in the corresponding media; and n_1 and n_2 are the refractive indices of mediums.The refractive index of tissue is a substantial parameter in determination of its optical response. Based on the reports in the literature, the index of refraction, n, for tissue generally ranges from 1.35 to 1.55 [32].

2.2 Absorption

Light is absorbed by chromophores in tissue. Each chromophore has its specific absorption spectrum that defines the level of absorption at each wavelength [33].

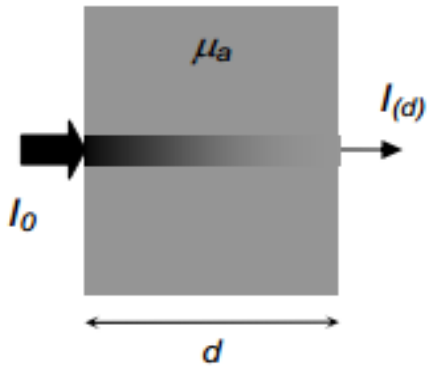

Figure 2.2 Attenuation of light through a non- scattering medium.

Source: [33].

Figure 2.2 depicts the attenuation of light through a non-scattering medium.

The transmitted light intensity through a homogeneous and non-scattering medium defined as

$$I_{(d)} = I_0 . e^{-(\mu_a . d)} \tag{2.3}$$

Where μ_a represents the absorption rate of medium (mm^{-1}) at a particular wavelength, d represents the thickness of the medium, and $I_{(d)}$, I_0 denotes the transmitted light intensity and incident light intensity respectively. The transmittance T is defined as the ratio between the transmitted light intensity and incident light intensity.

$$T = \frac{I_{(d)}}{I_0} \tag{2.4}$$

Similarly, absorbance A is defined as the loss in the light intensity and it is measured in units of optical density (OD) [33].

$$A = log_{10}\left(\frac{1}{T}\right) = log_{10}\left(\frac{I_0}{I_{(d)}}\right) = k.d \tag{2.5}$$

Where

T= Transmittance,

I_0= Incident light intensity,

$I_{(d)}$= Transmitted light intensity,

d= Optical path length,

2.3 Scattering

As the light interacts with medium, it changes its direction if the medium has scattering property. Thus, the photons don't propagate directly and this process is defined as scattering. Light scattering in tissue is determined by many variables such as the size of the scattering matter, the wavelength of the light, and the changes in the refractive indices of different tissues and their components (e.g. cell membranes and organelles) [33].

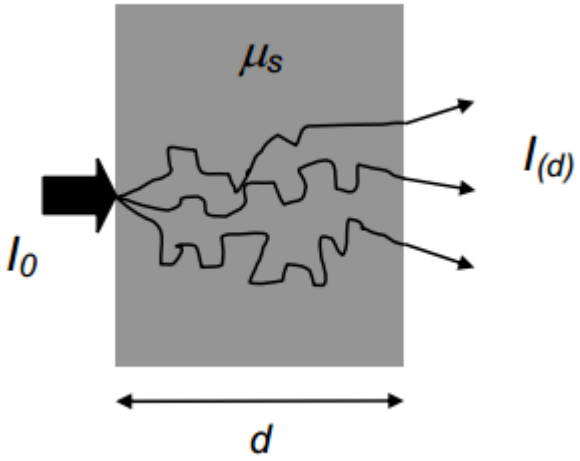

Figure 2.3 Attenuation of light through a scattering medium.

Source: [33].

There are two main types of scattering event, elastic scattering and inelastic scattering [34]. Elastic scattering occurs when the frequency of the incident wave is equal to the frequency of scattered wave. On the other hand, inelastic scattering occurs when the frequency of the incident wave is different than the frequency of the scattered wave [34]. Similar to the absorption, the non-scattered light intensity $I_{(d)}$ is defined as

$$I_{(d)} = I_0 . e^{-(\mu_s . d)} \tag{2.6}$$

Where d denotes the medium thickness and I_o denotes incident light intensity.

2.4 Absorption Properties of Tissue Components

As stated earlier, when the light interacts with tissue, it is absorbed by the tissue chromophores and absorbed light is converted to heat. Most of the biological soft tissues have low light absorption property in the visible and NIR wavelengths, especially between 600-1300 nm [35]. This spectral range is also known as "tissue optical window" or "therapeutic window". The main absorbing chromophores in the tissues are water, body fats, enzymes, melanin, and hemoglobin [4].

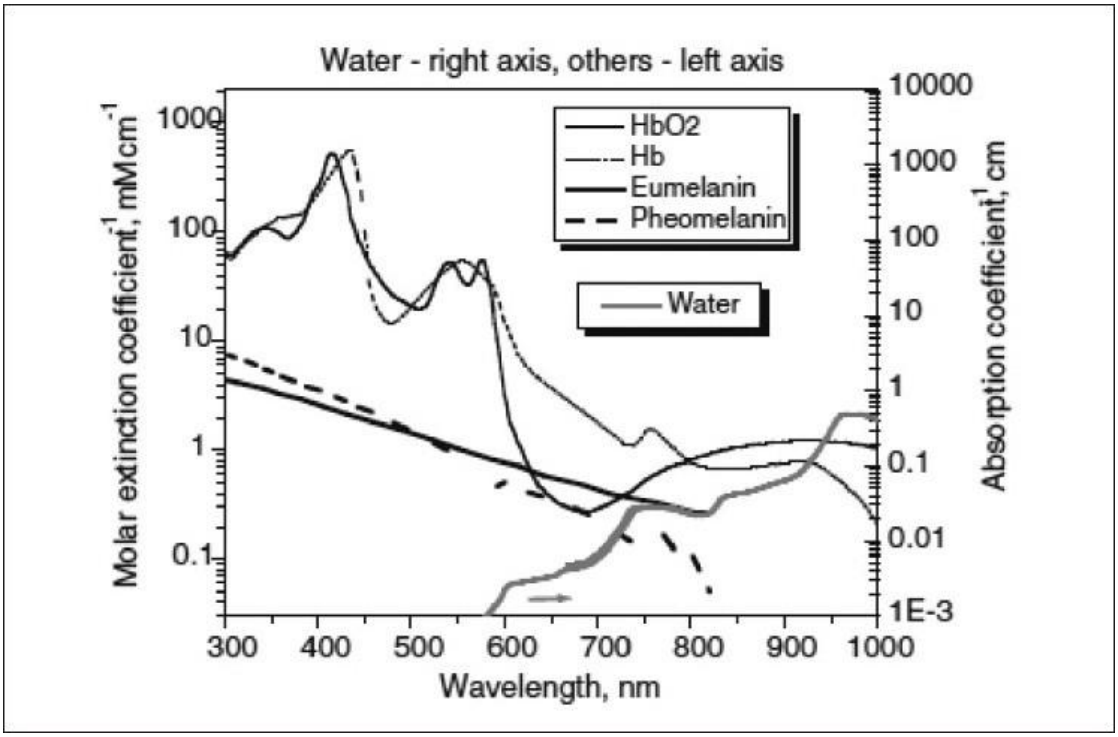

Figure 2.4 The absorption spectra for the main chromophores found within tissue. Hb: Hemoglobin. HbO2: Oxygenated hemoglobin.

Source: http://www.ijdvl.com/articles/2011/77/3/images/ijdvl_2011_77_3_349_79728_f7.jpg, (accessed April 16 2013).

At the shorter wavelengths, hemoglobin, oxygenated hemoglobin, and melanin are the main absorbers in tissue. Their absorption rate starts decreasing at 600 nm where the tissue optical window starts. As the figure shows, the absorbance values of the chromophores are relatively low when compared to the wavelengths out of the tissue

optical window. Due to the low absorption rate, less light intensity is needed in this window, and this yields to less thermal damage and other light tissue interactions.

In the tissue optical window scattering is dominant over absorption [33]. However, at the NIR region has lower scattering property than the visible region [35]. Due to this property NIR region is used to make non-destructive measurements on biological tissues. Moreover, the concentrations of static absorbers (i.e. water and melanin) and the dynamic absorbers (hemoglobin etc.) could provide useful information about the tissue structure.

2.4.1 Water

Water is one of the most important chromophores in tissue due to its high concentration in biological tissues. The water concentration in tissue is generally considered as a constant since it acts as a fixed constant absorber [36]. Figure 5 shows the absorption spectrum of pure water at 37 $^{\circ}$C. As seen in the figure, the water has a low absorption in the NIR range. After 900 nm, absorption increases rapidly with the increasing wavelength and peaks at around 970 nm.

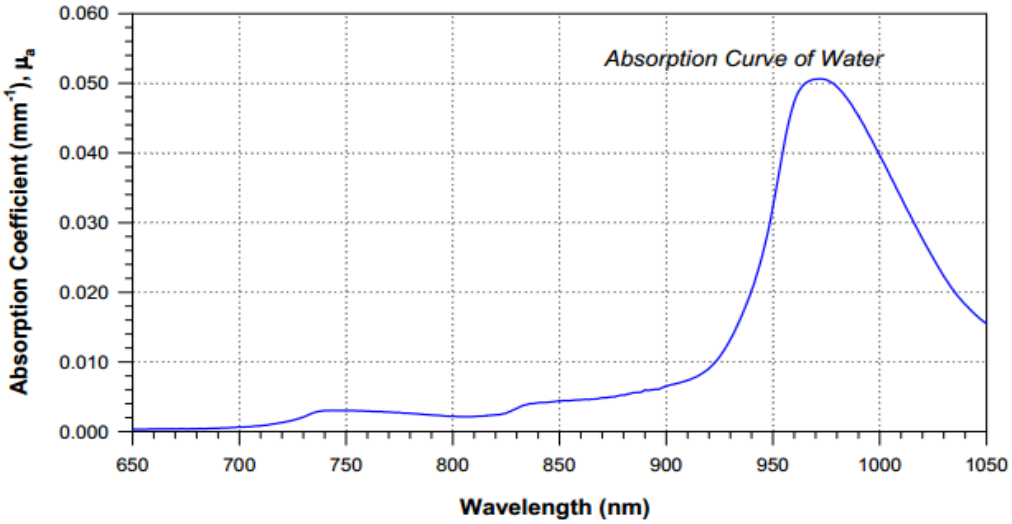

Figure 2.5 The absorption spectrum for pure water at 37 °C over the wavelength range from 650-1050 nm.

Source: [33].

2.4.2 Lipids

The lipids have also similar absorption characteristics to the water. They are also considered as a static absorber, since their concentration generally does not change during the measurements [36]. Figure 6 shows the absorption spectrum of pure pork fat between 650 nm and 1000 nm, which is thought to be similar to that of human lipids in muscle tissue.

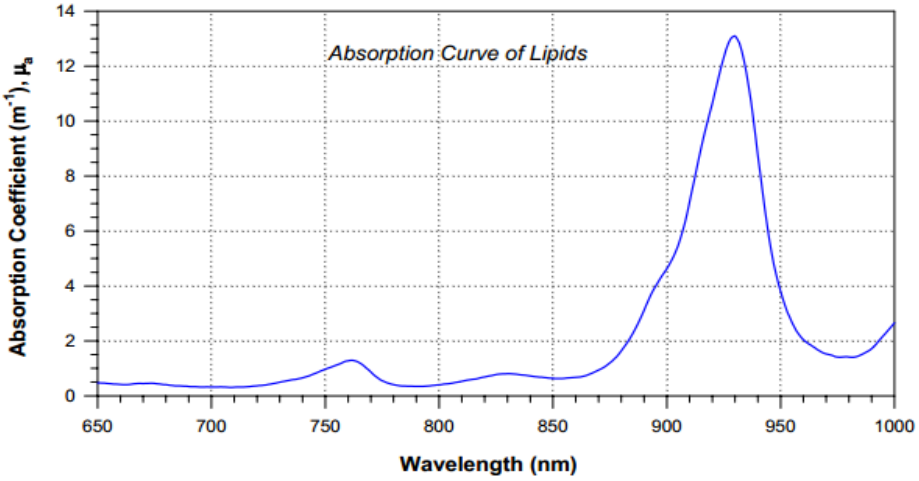

Figure 2.6 Spectrum of pork fat in the NIR range from 650 nm to 1000 nm.

Source: [33]

2.4.3 Hemoglobin

Hemoglobin has a major role in the delivery of oxygen from lungs to tissues (oxyhemoglobin), and transportation of carbon dioxide from the tissue (deoxyhemoglobin) back to lungs. Hemoglobin resides in the red blood cells, and carry 97% of the oxygen in the blood, remaining part is dissolved in the plasma [37]. Hemoglobin molecules are responsible for the absorption of light by blood. The absorption spectrum of hemoglobin molecules, deoxyhemoglobin and oxyhemoglobin, is given in figure 7. The absorption of oxyhemoglobin is relatively low when compared to deoxyhemoglobin between 650nm and 800nm. The isosbestic point is defined as the point where the absorption spectra of deoxyhemoglobin and oxyhemoglobin cross [33]. To sum up, oxygen saturation of blood effects the optical properties of blood.

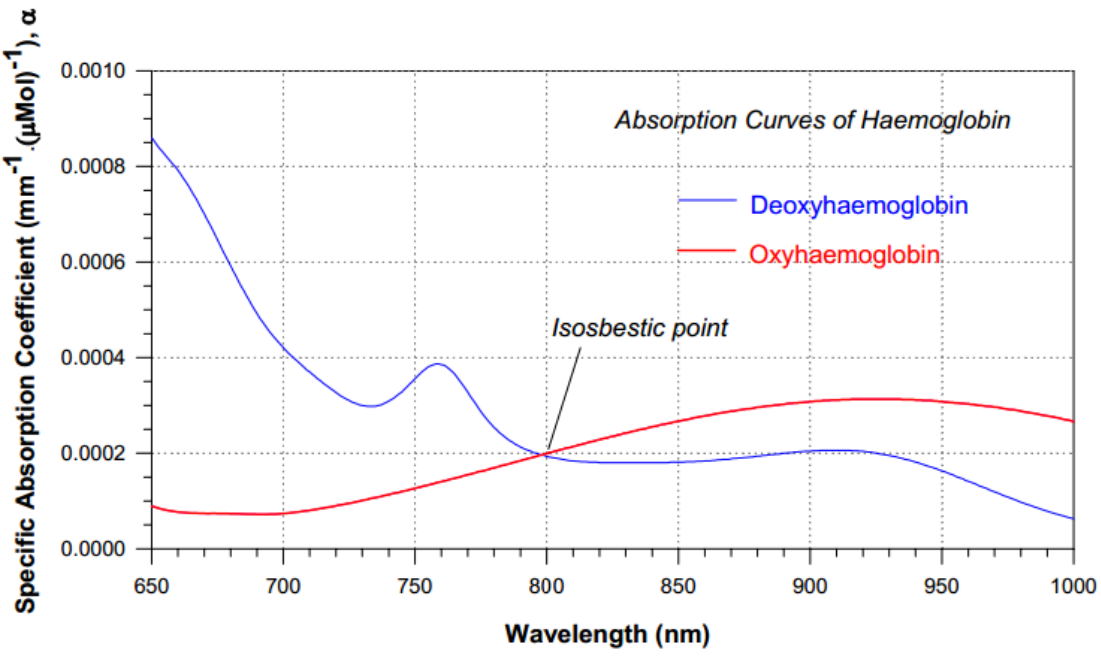

Figure 2.7 Absorption spectra of hemoglobin.

Source: [33]

2.4.4 Skin

The skin covers the whole body and provides protection to internal organs from environment. The skin is a turbid medium, where the blood and pigment content are distributed heterogeneously. Figure 8 shows the anatomy of the skin. The skin has three main layers that are:

- *Epidermis*: is the top layer of the skin, and comprised of millions of dead skin cells. Epidermis has a thickness of 100 μm, contains melanin pigment, and does not have any blood vessels [38].
- *Dermis*: is the underlying connective tissue, which is composed of nerves, blood vessels, sweat glands, and hair follicles [33]. The thickness of the dermis ranges from 1- 4 mm [38].
- *Hypodermis*: is located under dermis and contains subcutaneous adipose tissue. The thickness of hypodermis ranges from 1 to 6 mm [38].

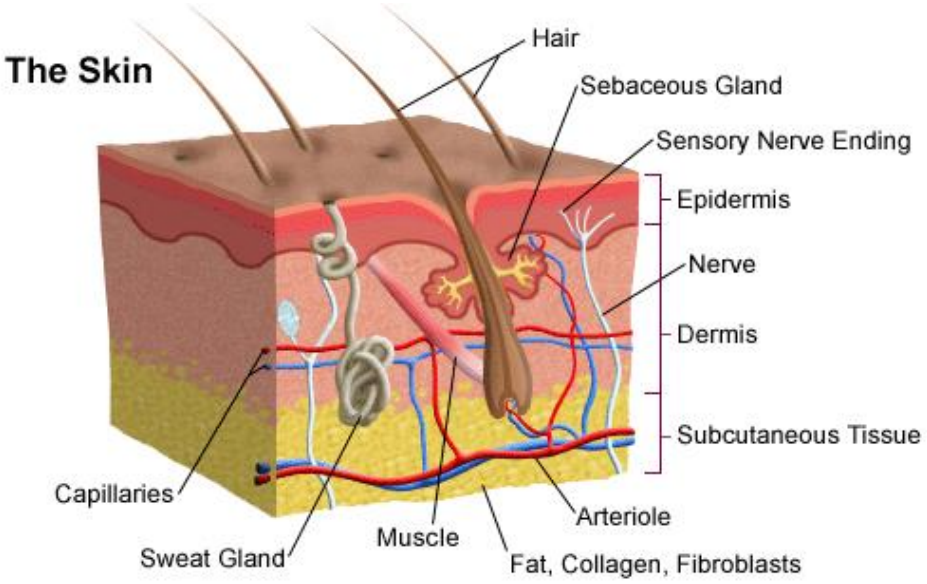

Figure 2.8 The anatomy of skin.

Source: http://childrenshospital.org/az/Site784/Images/SKINANATOMY.gif, (Accessed March 28 2013)

In the epidermis layer, light is absorbed and scattered mostly by the melanin pigments. Moreover, in the dermis layer, absorption and scattering are dependent on different chromophores due to its structure. In the visible range light is mostly absorbed by hemoglobin, carotene, and bilirubin; on the other hand in the IR range, the absorption is determined by water [38]. The scattering properties of the dermal layers are determined mostly by the fibrous structure of the tissue. Table 2.1 presents the data from Simpson et al work which probed the optical coefficients of human dermis [39]. According to the Table 2.1, one can say that the pigmentation of the skin effects the transmission of light through skin. As seen in Table 2.1 scattering is mostly responsible for the attenuation of the propagating light in skin. Another important point is the scattering decreases with the increasing wavelength due to the interaction between the particle size and photons.

Table 2.1 Summary of absorption and transport scattering coefficients of various tissue types.

Tissue	Wavelength (nm)	$\mu_a(mm^{-1})$	$\mu_s(mm^{-1})$
Caucasian dermis (n = 12)	633	0.033 ± 0.009	2.73 ± 0.54
	700	0.019 ± 0.006	2.32 ± 0.41
	900	0.013 ± 0.007	1.63 ± 0.25
Negroid dermis (n = 5)	633	0.241 ± 0.153	3.21 ± 2.04
	700	0.149 ± 0.088	2.68 ± 1.41
	900	0.045 ± 0.018	1.81 ± 0.040
Sub dermis (n = 12)	633	0.013 ± 0.005	1.26 ± 0.34
	700	0.009 ± 0.003	1.21 ± 0.32
	900	0.012 ± 0.004	1.08 ± 0.27

Source: [39]

CHAPTER 3

OPTICAL EMITTERS AND DETECTORS

3.1 Optical Emitters

Broad selection of light sources can be found in the market. Explanation of every light source will yield to series of books. In this thesis, only the most common semiconductor photoemitters will be discussed. Semiconductor photoemitters convert electrical signals into optical signals. The most common emitters are light emitting diodes, laser diodes, and vertical cavity surface emitting laser. These emitters will be discussed in the following sections.

3.1.1 Light Emitting Diodes

Light emitting diodes are semiconductors that convert electrical energy into light energy. LEDs contain PN junctions in their internal structure and when a sufficient forward voltage is applied to the leads of the LED, it will emit light in a range of specific wavelengths based on the material. LEDs have the advantages of low cost and long lifetime compared to laser diodes. Moreover, LEDs are being manufactured in various types; miniature, high power, and custom designs; and the wavelength selection are very broad. The advantages of LEDs can be listed as, small size, long life time, low cost, dimming, broad wavelength selection, wide availability, and relatively safe compared to other photo emitters.

3.1.2 Laser Diodes

Laser diodes are semiconductor lasers which have p-n junction and they are electrically pumped. They generate a very narrow spectral bandwidth, and shorter pulse durations than LEDs; and they are small in size, and very efficient.[40]. Laser

diodes can emit high light intensities compared to the LEDs. The light output of the laser diode is collimated since the emission area is very small, in micrometer range [40]. The applications of laser diodes include communication, disk players, printing systems, medical field. They are also used as pump sources for solid-state lasers (mainly Nd:YAG) [8].

Figure 3.1 Laser diodes.

Source: http://www.wavespectrum-laser.com/admin/infofiles/files/images/000000117.png, (accessed March 28, 2013)

3.1.3 Vertical Cavity Surface Emitting Diode Lasers (VCSEL)

Vertical-Cavity Surface-Emitting Diode Lasers (VCSELs) are recently developed semiconductor lasers. As the name of the laser states that, VCSEL emits light perpendicular from the top surface, on the other hand the conventional semiconductor emitters produce the light from the edges [41].

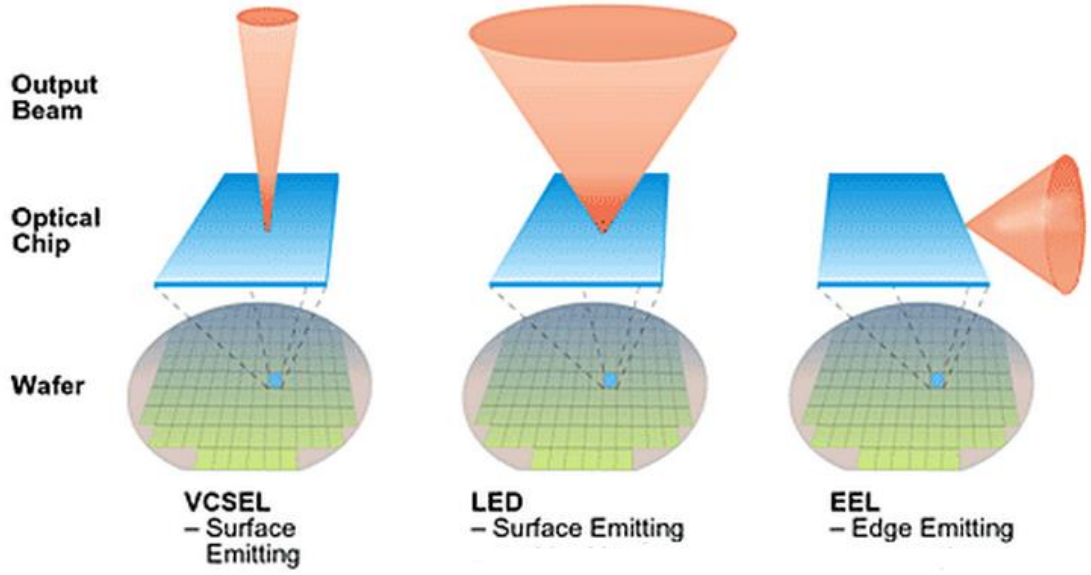

Figure 3.2 The comparison of output beam shapes of VCSEL, LED, Edge emitting lasers.

Source: [42]

VCSELs advantages could be listed as; wavelength stability and uniformity, high power output, and the beam quality [41]. VCSELs find applications in optical communications, pumping solid state lasers, and most recently in the medical field [41]. However, to operate VCSELs at high powers, there is a need for special drivers and specific heat sinks. Due to the market availability, cost of a VCSEL system is higher than the previous emitters. Moreover, since VCSEL emits highly collimated light intensities, it requires careful operation due to the safety reasons.

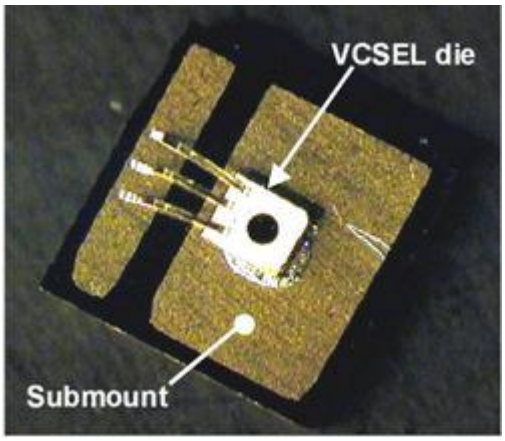

Figure 3.3 Package of high power VCSEL device.

Source: [41].

3.2 Light Detectors

Light detectors detect the electromagnetic radiation in the spectral region of light. Again, since there are too many light detectors only some of them which are used in medical applications will be discussed.

3.2.1 Photodiode

Photodiodes are semiconductor photosensors that generate a current or voltage when the PN junction is irradiated by light. Photodiodes are preferred due to their features such as; excellent linearity with respect to incident light, low noise, low cost, wide spectral response range, and long lifetime [43]. Generally, photodiodes have two operating modes: *photoconductive* mode and *photovoltaic* mode (Figure 13). In the photoconductive mode the LED a bias voltage is applied to the photodiode, whereas, in the photovoltaic mode, the bias voltage is not applied. Since there is no bias voltage in the photovoltaic mode, the photodiode acts as a current source and the current generated by photodiode is quite linear with respect to the incident light level [43]. In the photovoltaic mode; dark current, which is the current that flows through the photodiode in the absence of light, is not a problem, thus the only consideration is

thermal noise [44]. However, there are some disadvantages of this mode such as, slow response due to the large junction capacitance, and the responsivity to longer wavelength is relatively less [44]

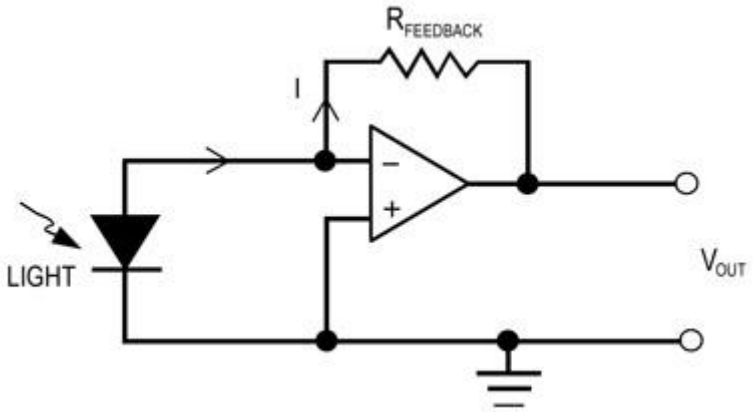

Figure 3.4 Photovoltaic mode operation of photodiode.

When a reverse bias voltage is applied to the photodiode, it operates in the photoconductive mode. The advantages of this mode are; shorter rise time, lower series resistance, lower junction capacitance, and the linear response over a wide range of light intensities [44]. However, due to the reverse bias, dark current is introduced noise levels also increase, and excessive reverse could damage the photodiode permanently [43, 44].

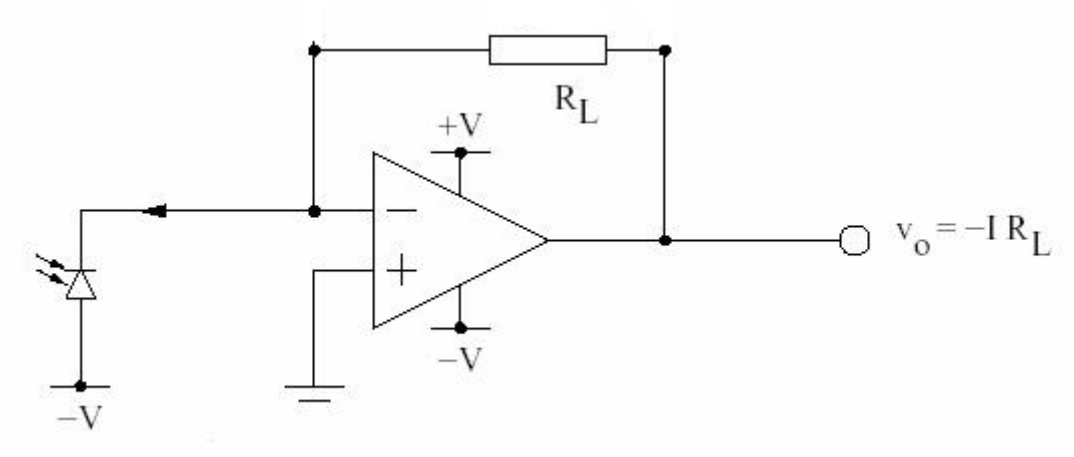

Figure 3.5 Photoconductive mode operation of photodiode.

3.2.2 Phototransistor

Phototransistors convert light into electricity in a similar fashion to the photodiodes. They can provide current gain due to their structure and this yield to much higher sensitivity [44]. The phototransistor operates same as the conventional transistor except the base current is provided by the incident light. The circuits with phototransistors are designed same as the regular transistor circuits. However, the phototransistors are slower than the photodiodes, and require external circuitry to operate.

3.2.3 Photoresistor

A photoresistor changes its resistance according to the light intensity. Photoresistors require external power source since it does not generate photocurrent. The internal material of photoresistor has high resistance in darkness, thus the applied voltage will generate small current. As the light absorbed by the material the resistance of the material reduces and current flowing through the device increases.

CHAPTER 4

METHODS

4.1 System Overview

The system is comprised of three main parts; electronic, optical, and mechanical. The electronic part, is responsible for generating an adjustable LED or laser pulse, driving the light source, and amplifying the photodiode output. Optical part comprised of two plano-convex lenses to focus the light beneath the tissue and the mechanical part consists of two micromanipulators and additional mechanical parts in order to move light source and tissue sample independently. Figure 4.1 shows the system block diagram. The details for each component will be given in the following sections.

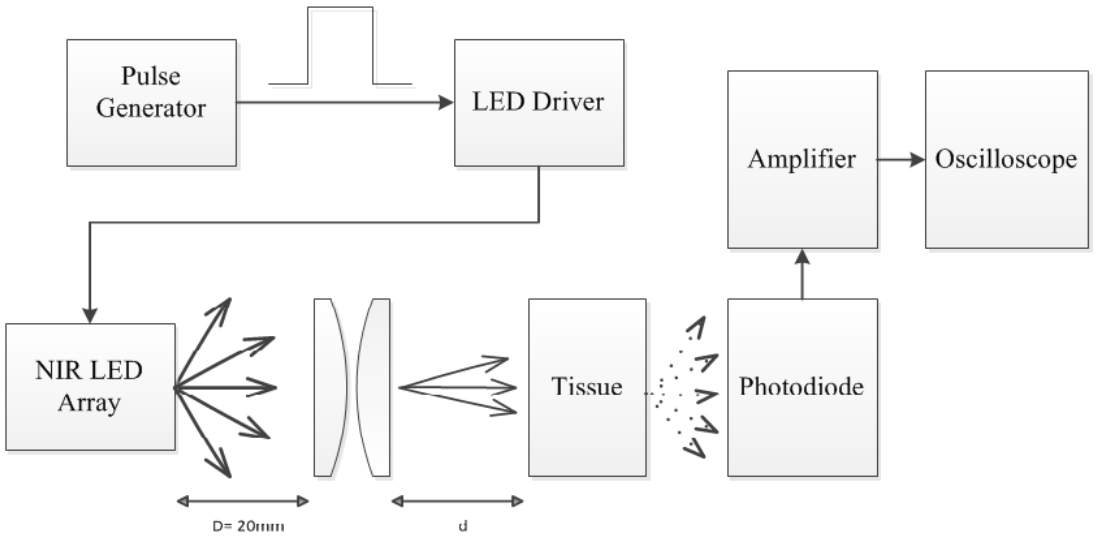

Figure 4.1 System block diagram.

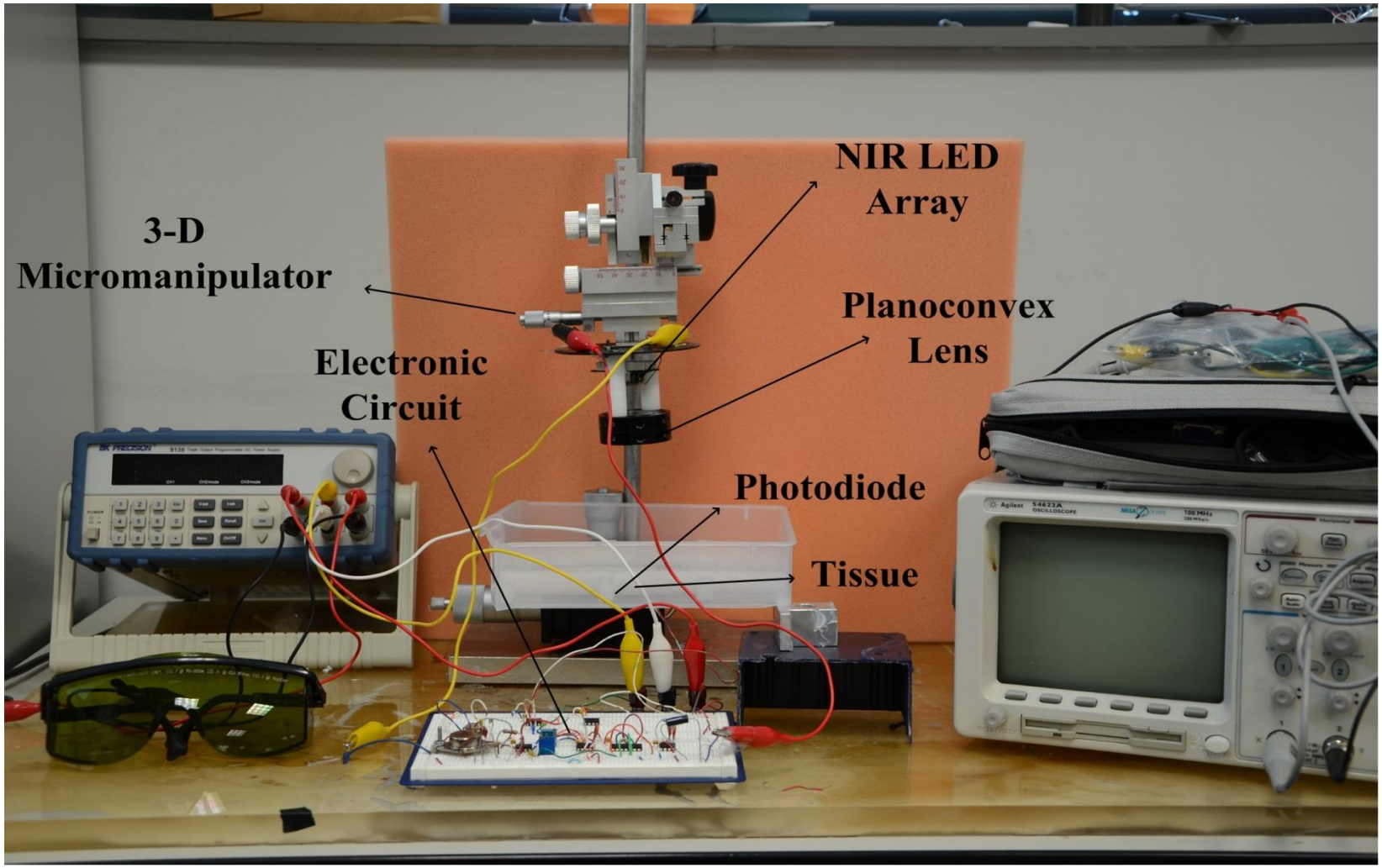

Figure 4.2 Experimental Setup

4.2 Electronic Circuit

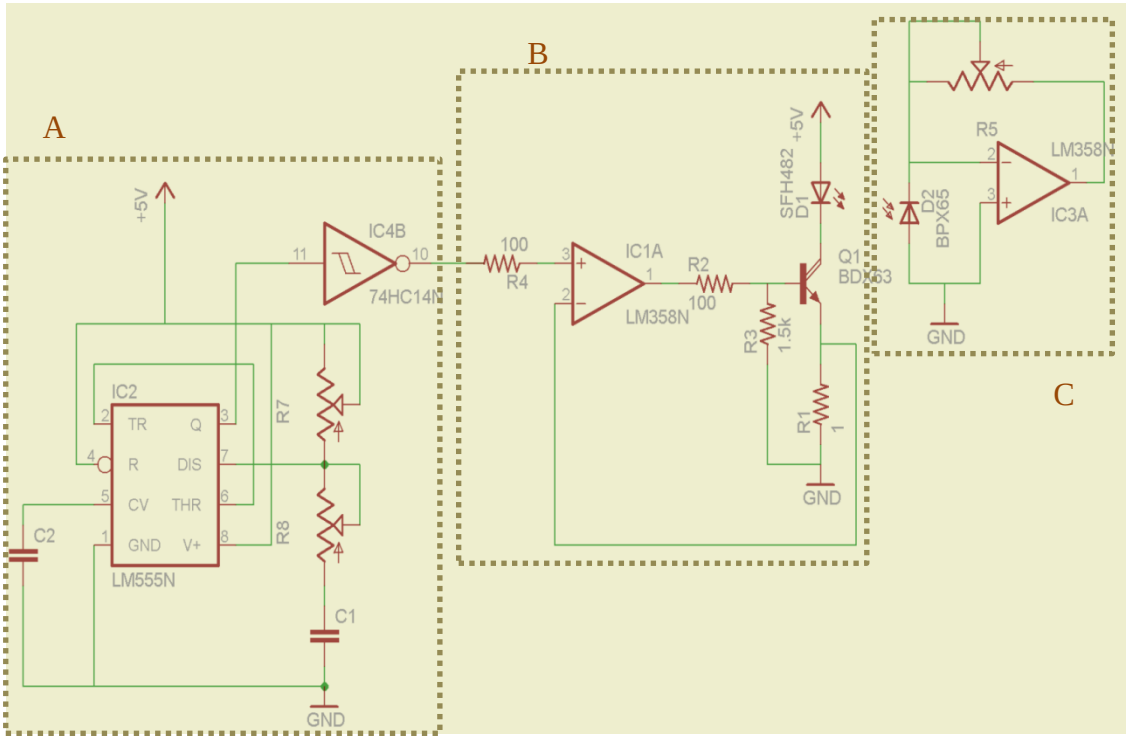

Figure 4.3 The schematic of the electronic circuit that was built to generate adjustable pulse, to drive LED, and to amplify the output of the photodiode. A) Pulse generator B) LED Driver C) Receiver circuit

4.2.1 Light Source

In this study, Enfis Uno Tag Infra-Red LED array (Photon Star LED, UK) was used as a light source.

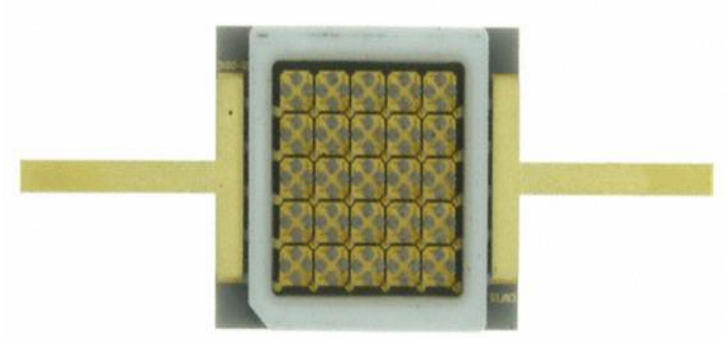

Figure 4.4 ENFIS UNO TAG NIR LED array.

Source: http://elcodis.com/photos/8/31/83128/enfis_un0_tag_array_uva.jpg, (accessed March 28 2013)

Enfis Uno Tag Array has its peak wavelength at 870 nm which is in the tissue optical window, where the absorption and scattering coefficients are relatively low. It has a 4500 mW typical power, 0.5 cm^2 aperture, and 9000 mW/cm^2 output power density [45]. Besides the wavelength, LED Array was selected as a light source due to its ease of operation, safety reasons and cost.

4.2.2 Light Sensor

Photodiode was selected as a light sensor. A photodiode was chosen due to its characteristics such as working without external power (photovoltaic mode), small size and high responsivity.

Figure 4.5 MTD3010PM photodiode.

Source: http://media.digikey.com/Photos/Marktech%20Optoelectronics/MFG_MTD3010PM.jpg, (accessed March 28 2013)

The MTD3010PM (Marktech Optoelectronics, USA) photodiode was used in our system. MTD3010PM has peak sensitivity wavelength at 900 nm where it has the highest responsivity, 0.58 A/W [46]. As the Figure 4.3 shows that at 870 nm, selected photodiode has a responsivity of nearly 0.58 A/W, which implies that the emitted light will be detected efficiently. Additionally, MTD3010PM has a wide angular response, ± 60 degrees, which means that most of the emitted light will be detected by the photodiode.

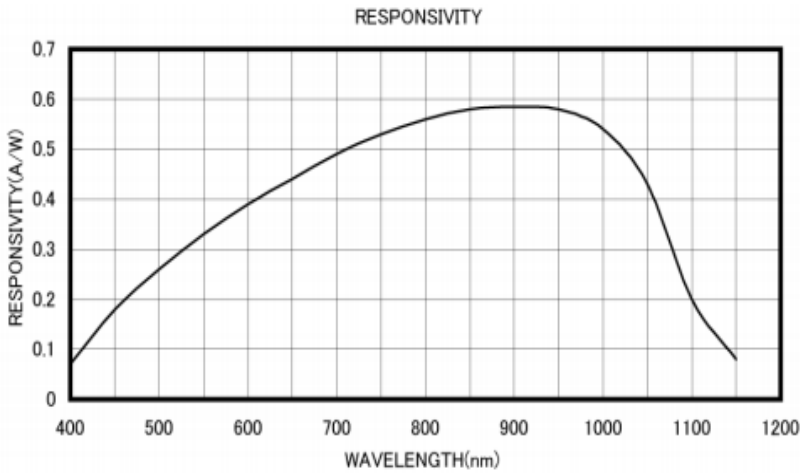

Figure 4.6 Responsivity curve of MTD3010PM [46]

4.2.3 Timing Circuit

The required pulse to drive the LED array was generated by using LM 555 Timer (Texas Instruments, USA). The LM555 is highly stable when generating accurate time delays or oscillations. The output of the LM 555 timer can source or sink up to 200 mA.

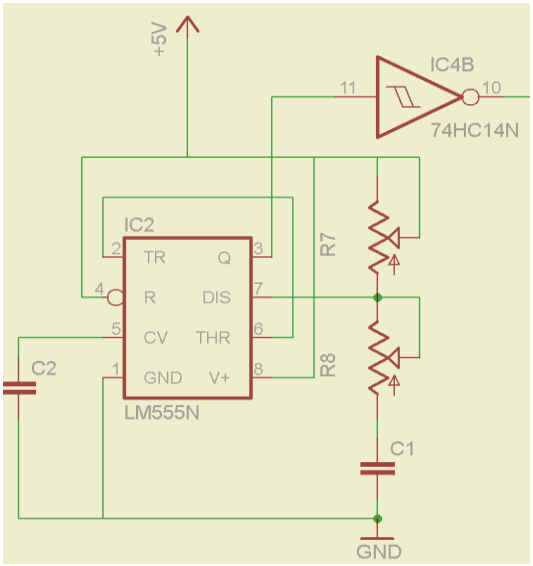

Figure 4.7 Pulse generator circuit.

The astable configuration of LM 555 was used to generate pulses. The capacitor value was selected as 1 µF, and two trim pots (1 kΩ, 50 kΩ) were used to adjust pulse width and the frequency of the output signal.

$$t_1(output\ high) = 0.693 * (R_7 + R_8) * C \tag{4.1}$$

$$t_2(output\ low) = 0.693 * (R_8) * C \tag{4.2}$$

$$T = t_1 + t_2 \tag{4.3}$$

$$Duty\ Cycle = \frac{On\ time\ (t_1)}{T} \tag{4.4}$$

The duty cycle of the output signal cannot go below 50% due to the internal characteristics of the timer. So, to achieve duty cycles less than 50% an inverting schmitt trigger, 74HC14 was chosen because of fast transition times. According to the equations 4.1, 4.2, and 4.3; the pulse width was adjusted to 200 µs and the period was adjusted to 33 ms (frequency 30 Hz).

The duty cycle of the generated signal was adjusted to 99.4% and the output was connected to the inverting Schmitt Trigger. The output of the Schmitt Trigger, which had a duty cycle of 0.6%, was connected to the driver circuit.

4.2.4 LED Driver

The output current of the LM 555 timer is not sufficient to drive the LED array directly, and connecting the output directly to the LED array could yield improper operation of LED array, or excessive current demands could damage the timer. Both for protection and better operation, there is a need for driver circuit to provide constant and sufficient current to the LED array. Figure 19 shows the driver circuit for LED array. The negative feedback to the inverting input forces the emitter and op-amp input voltages to be equal, thus keeps the LED current at a value defined by the input voltage and the emitter resistor by the Ohms law.

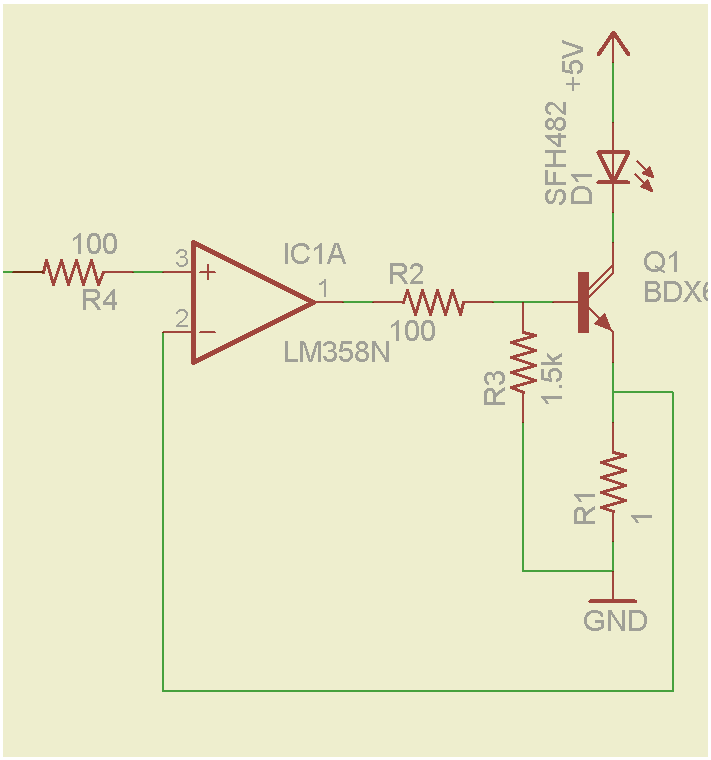

Figure 4.8 LED driver circuit.

Since the emitter current is almost equal to the collector current, LED current is defined as;

$$I_{LED} \approx \frac{V_e}{R_e} \tag{4.5}$$

4.2.5 Receiver Circuit

The current output of the photodiode in photovoltaic mode is very small. In order to detect the current output of photodiode, there is a need for amplification. Transimpedance amplifiers are used for this purpose usually which basically convert current to voltage.

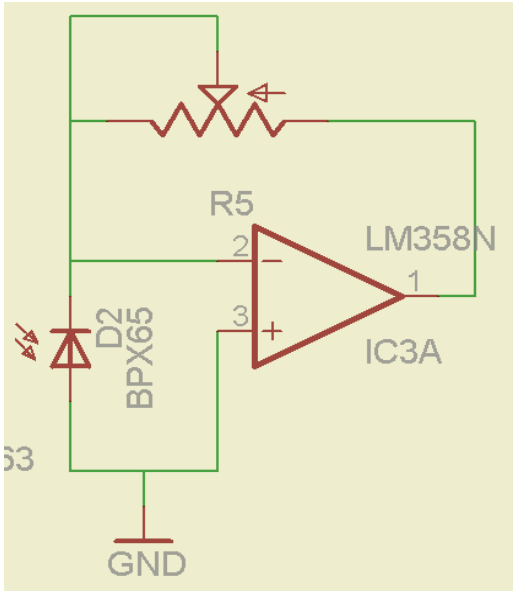

Figure 4.9 Photodiode transimpedance amplifier.

Figure 4.7 shows the transimpedance amplifier that was used in our circuit. Note that the photodiode was operating in the photovoltaic mode. The potentiometer adjusts the gain.

4.3 Experimental Procedure

As a replacement of human tissue, pork rib end roast was purchased from a vendor and due to its similar optical characteristics to human tissue [47]. Pork tissue was cut into slices that have approximately 2 cm thickness. All the parts except one, which was used for the first experiment, were put into sealed bags and kept in the freezer. The sliced pork tissues were placed between two glass plates to measure their thickness. Then, the investigated tissue was placed in a plastic container which has the MTD3010PM photodiode in the middle leveled with the bottom surface. Phosphate Buffered Saline (Sigma-Aldrich Company, USA) was added into the plastic container to prevent the tissue from drying.

First, to measure the output of the LED array and to create a profile of the LED light output, measurements were taken without tissue. These data were used while calculating the percent penetration values as the normalization value. The distance between LED array and the photodiode was adjusted to 1 mm while keeping them aligned. Then the LED array was moved along the x axis with 1 mm increments in both directions horizontally. The LED array light output is not collimated thus in order to focus under the tissue, two NT 45-504 plano convex lenses (Edmund Optics, USA) with a diameter of 25 mm and focal length of 25 mm, were placed between the LED array and the tissue.

Same measurements without tissue were taken in the same way for the LED array output with the lenses. The distance between the surface of the lenses and pork tissue was adjusted to 1 mm using the 3-D micromanipulators. Additionally, LED-lens assembly was aligned with the photodiode. After making the alignments, power was applied to the circuit and the penetrated light through the tissue was measured by

moving the LED-lens assembly in the x axis between -20 mm (left) to 20 mm (right) using the 3-D micromanipulators. The LED-lens assembly was moved with 1 mm increments in both directions and the voltage output of the transimpedance amplifier was measured using an oscilloscope. The gain of the transimpedance amplifier was adjusted using different values of the feedback (gain) resistors to quantify the output of the photodiode accurately. The photodiode current was calculated by dividing photodiode voltage by the feedback resistor.

After taking the light measurements with 20 mm thick pork tissue, the same tissue was cut down to a slice of approximately 19 mm thickness. The same procedures were applied to the 19 mm slice and the measurements were repeated. Same procedures were applied repeatedly until the tissue thickness was down to 1 mm, at which time the tissue sample was disposed. Previously sliced tissues were used respectively and same procedures were applied to measure the light penetration of each tissue.

In addition to the pork tissue, the optical properties of three types of rat tissue; i) skin from the back, ii) skin and muscle from the thigh, iii) skin and muscle from the abdominal area, were investigated. The sample size for the rat tissue was one for each kind and measurements were taken immediately after tissue extraction.

The incident irradiance was calculated according to equation 4.6. The responsivity of the photodiode was 0.58 A/W at 870 nm.

$$Incident\ Power(mW) = \frac{I_{pd}(mA)}{0.58\ A/W} \tag{4.6}$$

$$Irradiance(mW/cm^2) = \frac{Incident\ Power(mW)}{A_{photodiode}\ (cm^2)} \quad (4.7)$$

CHAPTER 5

RESULTS AND DISCUSSION

5.1 Results

The light output profile of the LED array is important when determining the transmittance of light through the tissue. Since the measurements were taken with the photodiode with a very small active area, it was important to determine the spatial distribution of light intensity while changing the position of the LED array in the x axis. Two different cases were investigated; 1) without lenses, 2) with lenses.

First, the optical power of LED array (without lenses) was measured while injecting 1.38 A through the LED. The total output power, measured with power meter, was 4.88 mW for a duty cycle of 0.6%, which corresponded to a peak power of 810 mW.

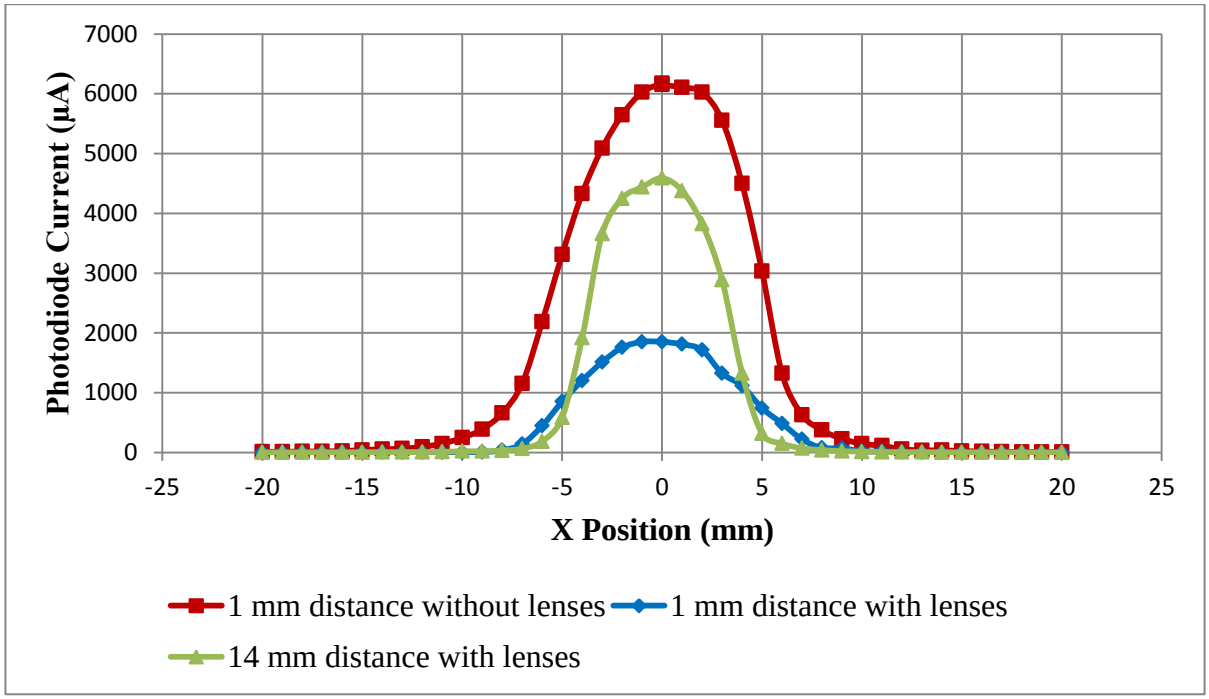

Figure 5.1 Photodiode current as a function of the relative position of the LED system with respect to the photodiode.

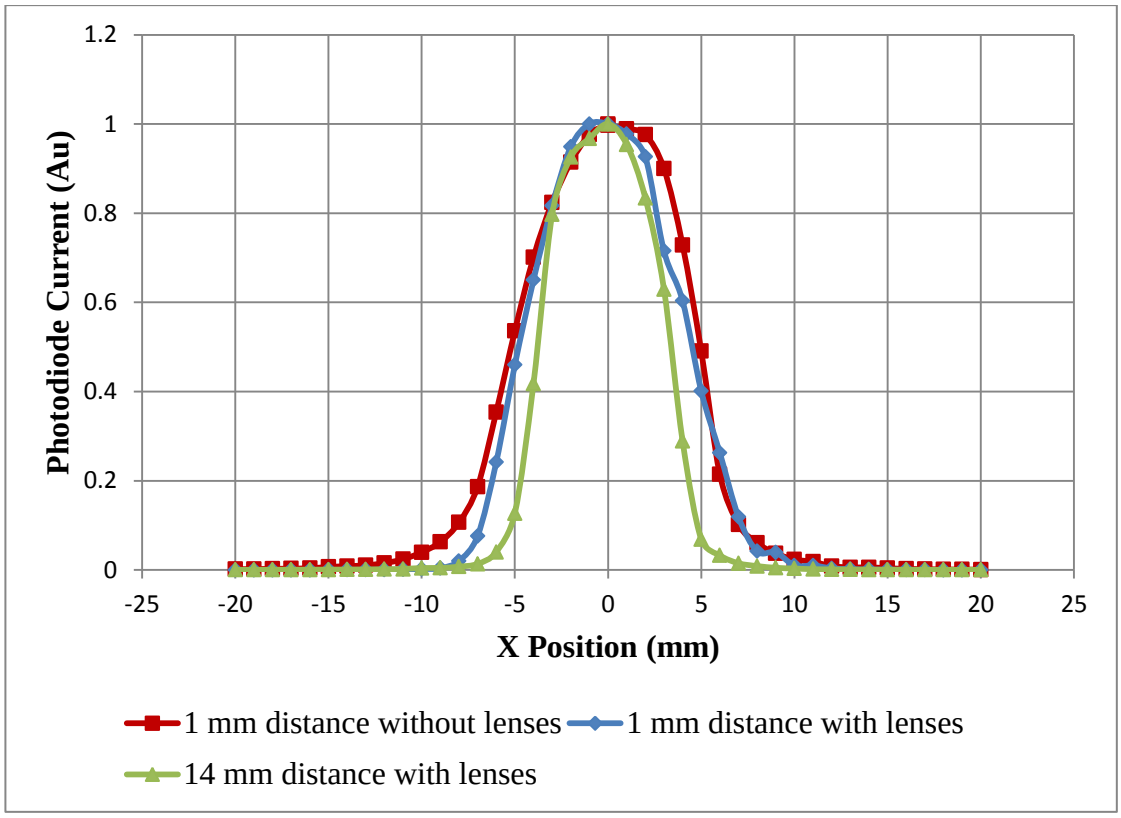

Figure 5.2 Normalized photodiode current values as a function of the relative LED position.

The line with square marker shows the profile of the photodiode current with respect to the x position. The distance between the photodiode and LED array was 1mm, and planoconvex lenses were not used. As seen on Figure 5.1, the photodiode current was 6.173 mA while the photodiode and LED array was aligned. According to the equation 4.6 the incident peak power and peak irradiance, which were detected by the photodiode in the middle (i.e., x position of 0), calculated as 10.64 mW and 472.88 mW/cm^2 respectively.

For the second step, planoconvex lenses were used to focus the light, and the distance between the photodiode and the lens surface was adjusted to 1 mm. The line with diamond marker shows the profile of the photodiode current as a function of the x position. The photodiode current was 1.85 mA; the incident peak power and corresponding irradiance were calculated as 3.19 mW and 141.77 mW/cm^2. It is

important to note that the detected peak power, therefore irradiance and current, were decreased with the use of planoconvex lens. Since there is a 2 cm distance between LED array and the other surface of the lens, all the light that was emitted from LED array, could not be collected by the lens. Moreover, although the selected planoconvex lenses have a coating to eliminate the reflection of VIS-NIR light, some of the photons that hit the lens surface were reflected. Additionally, the focal length of the planoconvex lenses is longer than 1 mm, so for the second case, the LED light was not focused properly at 1 mm, which results in signal loss.

The line with triangle marker shows the profile of the photodiode to LED-lens assembly distance of 14 mm. In order to find the actual focal length of the LED-lens assembly, the distance between the photodiode and LED-lens assembly was changed until the photodiode amplifier output was maximized. The maximum voltage value was detected at a distance of 14 mm. The photodiode current was 4.588 mA; the incident peak power and corresponding irradiance were calculated as 7.91 mW and 351.55 mW/cm^2. Even if the profile shows that the lens focused the LED light, the irradiance is still less than the first situation. The attenuation due to the reflection and wide angular output of LED are also applicable to this case. Figure 5.2 shows the normalized profiles for each case. Planoconvex lenses provided a narrower light profile due to their focusing property.

Figure 5.3 shows the photodiode current with respect to the x position for four different tissue thicknesses ranging from 4 mm to 9 mm. These measurements were taken with the planoconvex lenses and with a distance of 1mm between tissue and the lenses.

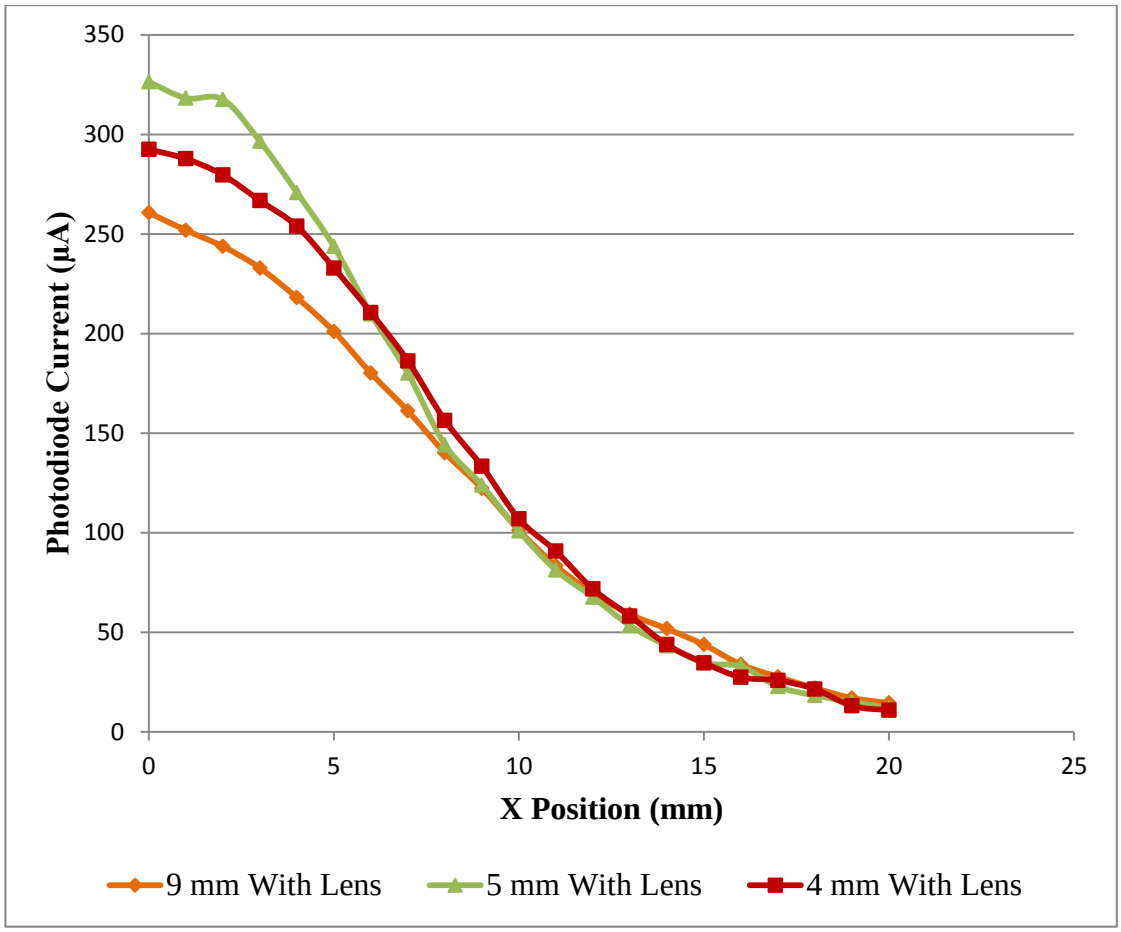

Figure 5.3 Spatial profile of the photodiode current for different tissue thicknesses from Sample 1.

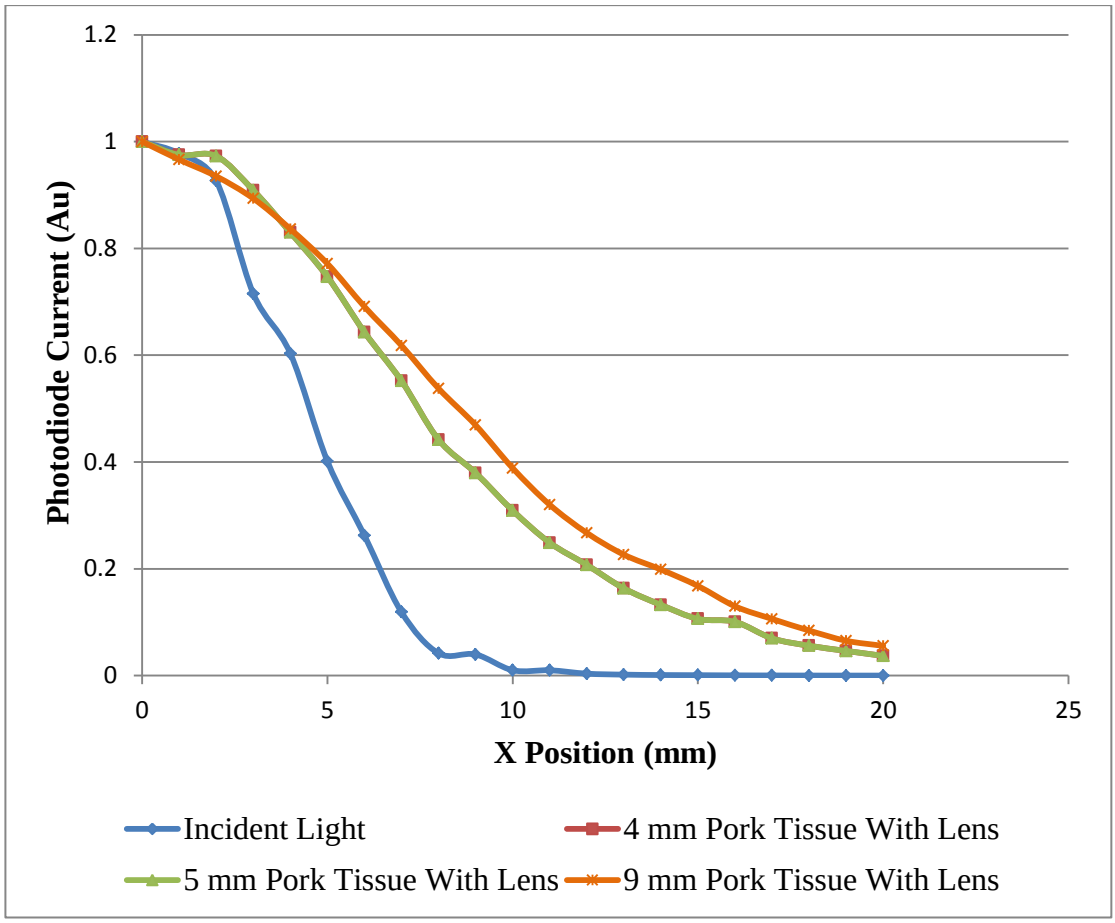

Figure 5.4 Normalized spatial profile of the photodiode current for different tissue thicknesses from Sample 1.

Table 5.1 Summary of the Measurement Results for Sample 1

Thickness	Incident Irradiance (mW/cm^2)	Detected Irradiance (mW/cm^2)	Detected Photodiode Current (μA)	Transmittance (%)
4 mm	141.77	22.41	292	15.8
5 mm	141.77	25.01	326	17.6
9 mm	141.77	19.97	260	14.1

As seen on Table 5.1, the photodiode current was highest at 5 mm, and the transmittance was found as 17.6 %. From Figure 5.4, we can say that 5 mm thick tissue has a relatively narrower spatial profile of photodiode current than the other tissue thicknesses.

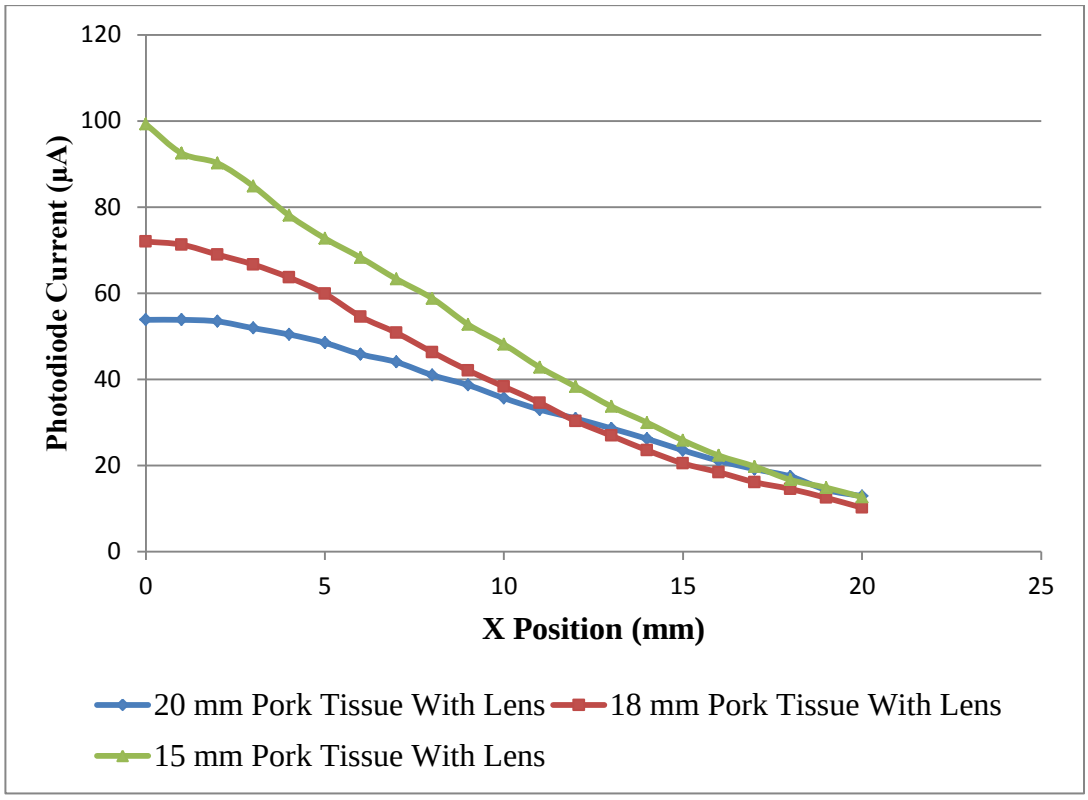

Figure 5.5 Spatial profile of the photodiode current from Sample 2.

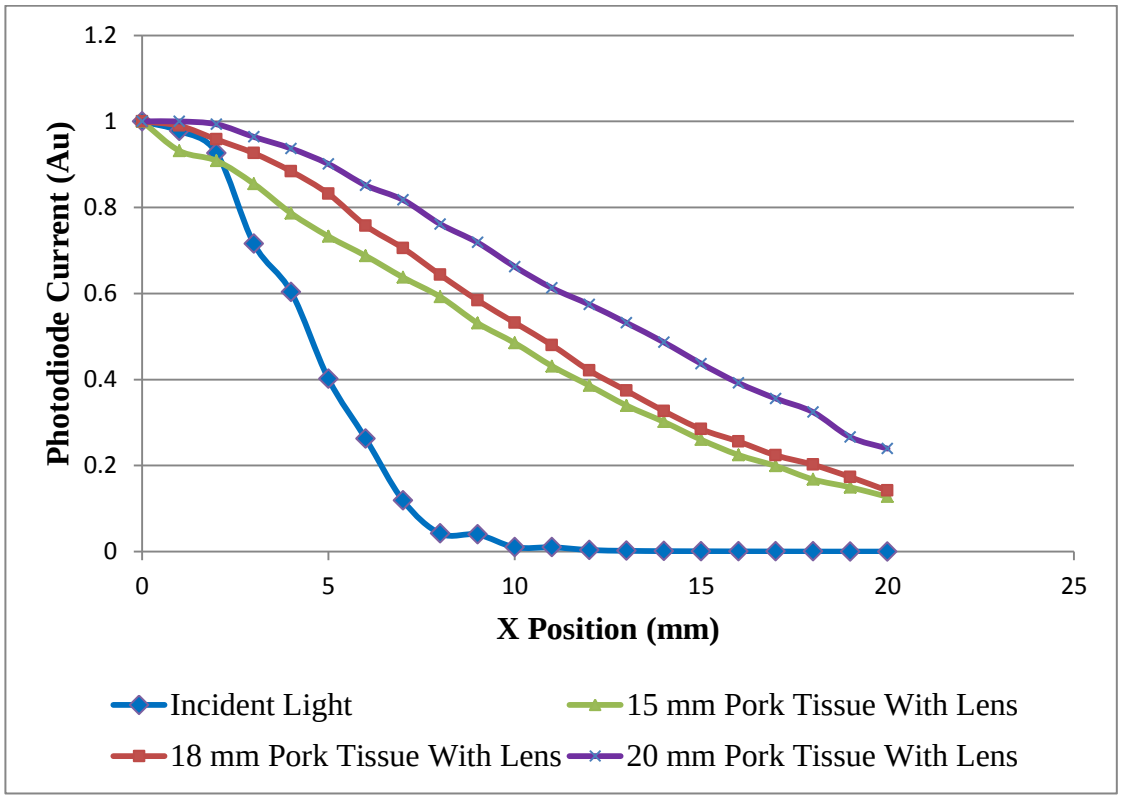

Figure 5.6 Normalized spatial profile of the photodiode current from Sample 2

The second sample measurements were started with 20 mm thick pork tissue. According to the Figure 5.6, at 15 mm tissue thickness, the focusing effect of planoconvex lens was relatively better than the other thicknesses.

Table 5.2 Summary of Measurements for Sample 2

Thickness	Incident Irradiance (mW/cm^2)	Detected Irradiance (mW/cm^2)	Detected Photodiode Current (µA)	Transmittance (%)
15 mm	141.77	7.60	99	5.3
18 mm	141.77	5.51	72	3.8
20 mm	141.77	4.12	53	2.9

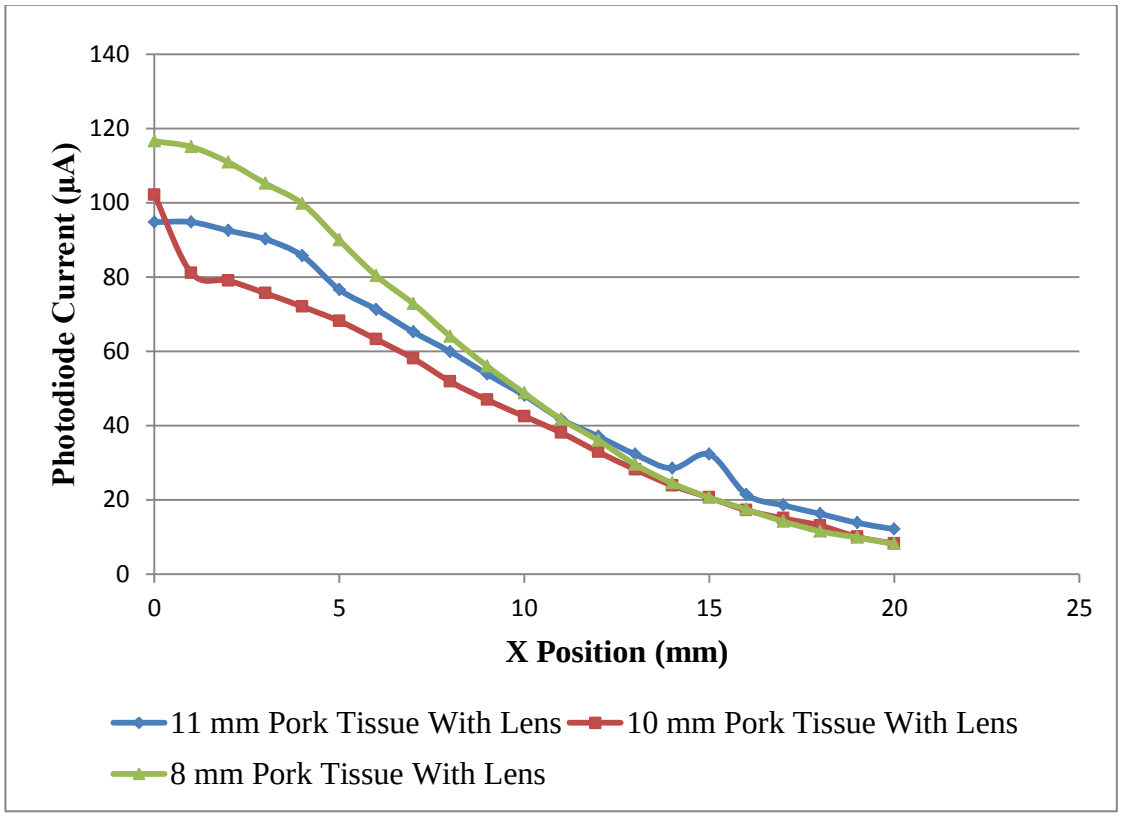

Figure 5.7 Spatial profile of the photodiode current from Sample 3

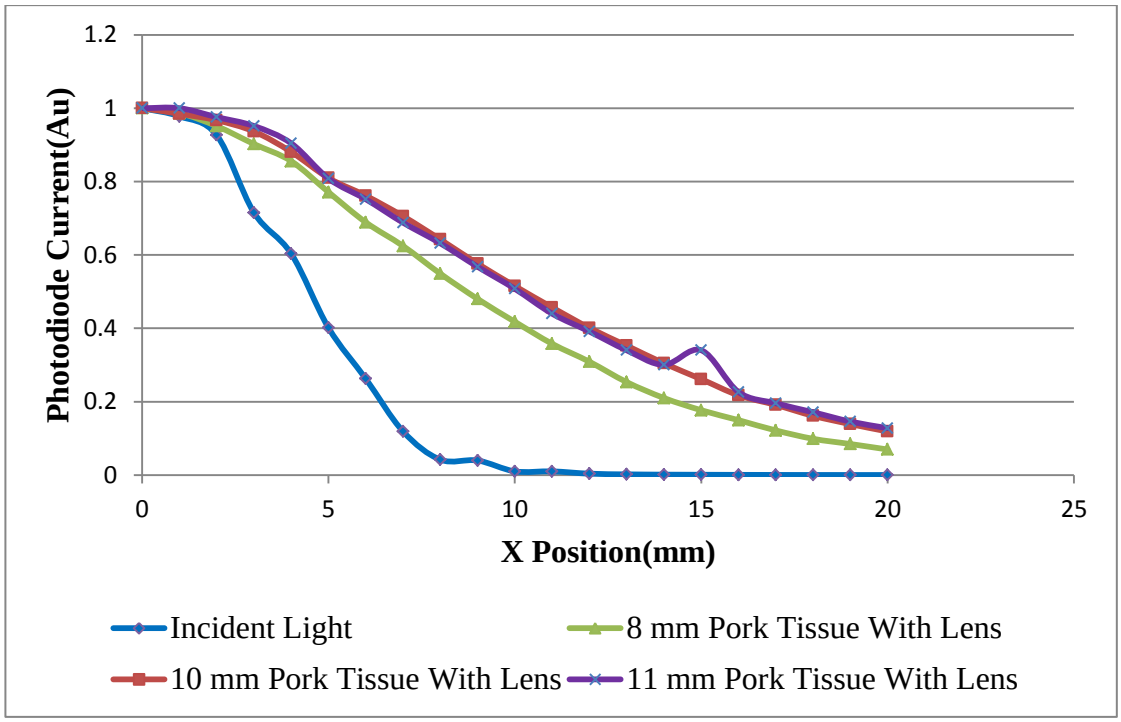

Figure 5.8 Normalized spatial profile of the photodiode current from Sample 3

Table 5.3 Summary of the Measurements from Sample 3

Thickness	Incident Irradiance (mW/cm^2)	Detected Irradiance (mW/cm^2)	Detected Photodiode Current (μA)	Transmittance (%)
8 mm	141.77	8.93	116	6.2
10 mm	141.77	7.82	102	5.5
11 mm	141.77	7.26	94	5.1

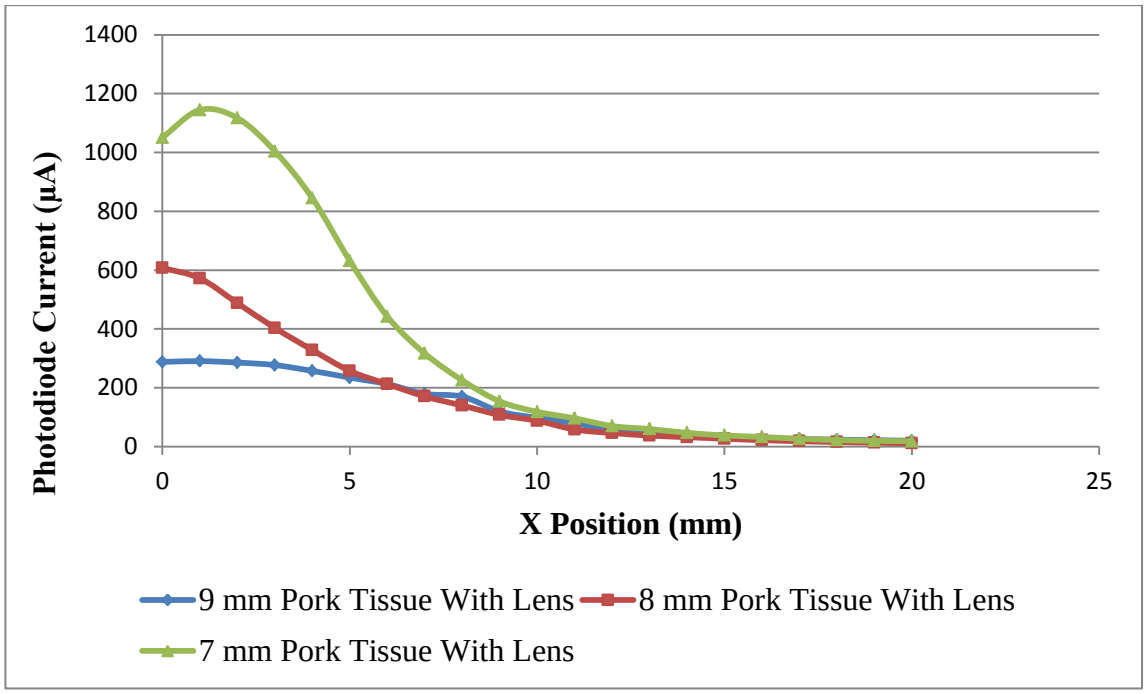

Figure 5.9 Spatial profile of the photodiode current from Sample 4. The distance with the tissue and lens was adjusted to detect maximum photodiode current. The distances for 9 mm, 8 mm and 7 mm pork tissues were 10 mm, 10 mm, and 12 mm respectively.

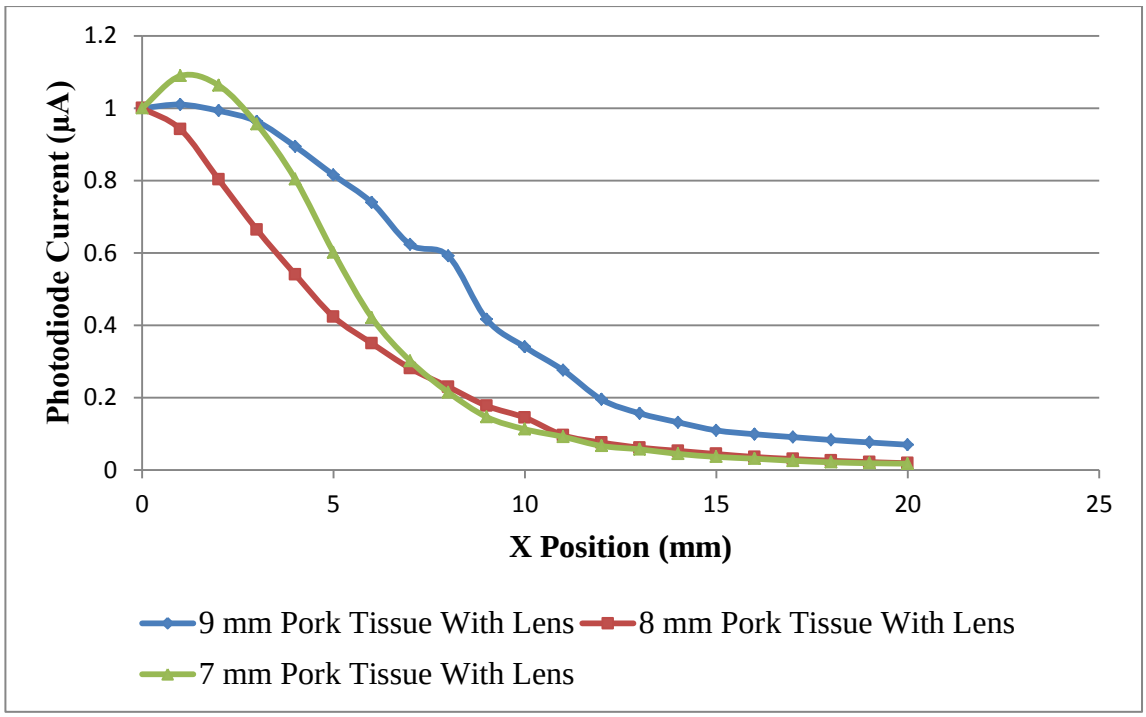

Figure 5.10 Normalized spatial profile of the photodiode current from Sample 4. The distance with the tissue and lens was adjusted to detect maximum photodiode current. The distances for 9 mm, 8 mm, and 7 mm pork tissues were 10 mm, 10 mm, and 12 mm respectively.

Table 5.4 Summary of the Measurements from Sample 4. Note that the distance between the lens and tissue is 10 mm, 10 mm and 12 mm for 9 mm, 8 mm and 7 mm tissue thickness respectively.

Thickness	Incident Irradiance (mW/cm^2)	Detected Irradiance (mW/cm^2)	Detected Photodiode Current (μA)	Transmittance (%)
7 mm	141.77	87.71	1144	61.8
8 mm	141.77	46.57	607	32.8
9 mm	141.77	22.28	290	15.7

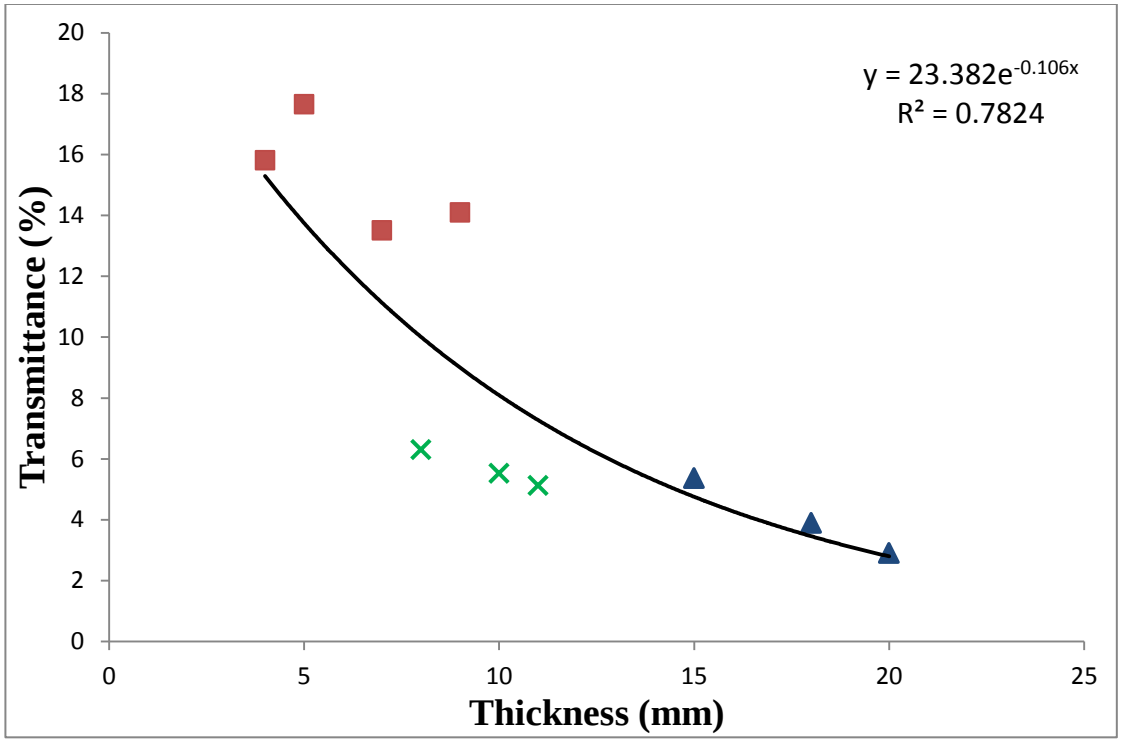

Figure 5.11 Total transmittance as a function of pork tissue thickness. Each marker represents a different tissue sample.

In addition to the transmittance measurements, the temperature elevation due to the NIR light illumination on the surface was investigated. Temperature elevation was detected by placing the thermocouple on the tissue surface. During the pork tissue measurements, a temperature increase of 1.2 °C was observed on the surface of the tissue slab.

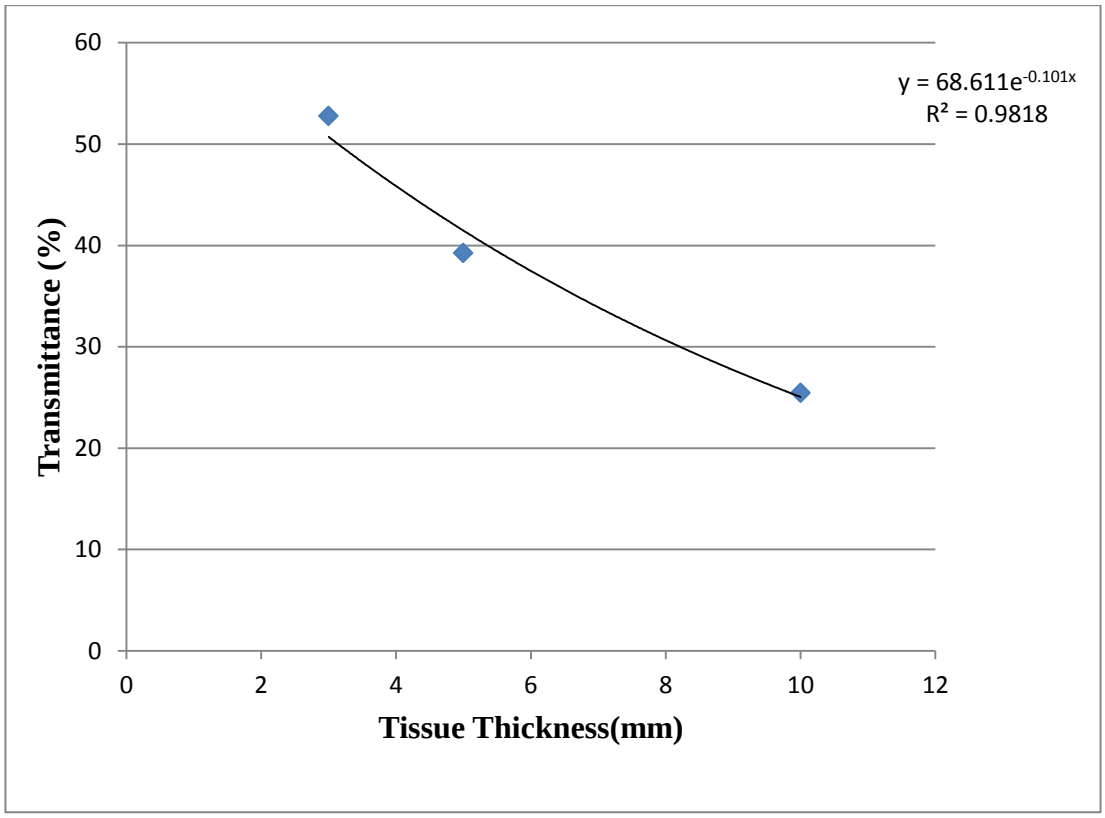

Figure 5.12 Total transmittance as a function of thickness for the rat tissues.

Table 5.5 Summary of the Measurements from Rat Tissues

Tissue Type	Tissue Thickness	Transmittance (%)
Skin	3 mm	52.7
Skin + Thigh	8 mm	39.2
Skin + Abdominal	9 mm	25.4

5.2 Discussion

The transmittance of light through tissue is determined by absorption, scattering and reflectance of the tissue components. In the NIR region the absorption and scattering by tissue is low, but it is not negligible. At the high end of NIR region, water limits the light transmission through tissue due to its high absorption rate [35]. Additionally, absorption by tissue chromophores such as fat, melanin, and hemoglobin is also responsible for the light attenuation.

From the normalized photodiode current figures, it can be seen that the spatial extent of the light is increased due to scattering. According to the equation 2.6, we expected to see an increase in the scattering with the increasing tissue thickness. The normalized photodiode current plots confirm this expectation. As it is mentioned earlier, in the NIR region, scattering is more pronounced than the absorption. The concentration of scattering particles, particle size and the refractive index mismatch affects the scattering, thus results in the decrease of transmittance.

The measurements were taken with the tissues bought from a local food vendor and the samples were not very homogenous. Thus, the difference between the optical properties of different samples contributed to the variance in the NIR light transmittance measurements. In addition we used saline to keep tissues moist. The saline on the surface of the tissue also introduced an additional medium between the incident light and tissue, and thus it reflected, absorbed, and scattered the incident light to small extent.

Many tissues are layered and consist of different constituents. Thus, determining the optical properties of tissue is very difficult. Many investigators have reported values for absorption and scattering coefficients that were not consistent with each other. The results varied due to the model assumptions, measurement techniques,

experimental setup, tissue extraction methods and calibration procedures [48]. For this reason, determining the total transmittance as a function of tissue thickness is more useful since it takes into account all of these factors.

Figure 5.11 clearly shows an exponential decrease in the transmittance with an increase in the tissue thickness. For thicknesses of 4 mm-20 mm, the transmittance ranges from approximately 18% to approximately 3%. Ackermann et al., used Yorkshire-cross farm pig dermal samples to investigate the NIR light transmittance through samples using 850 nm narrow band VCSEL. The total transmittance ranged from 27% to 5% of the total emitted power for tissue thicknesses of 1.5 mm-11 mm [19]. The difference in the wavelength, collimation of the light source, and the tissue type could be effective in the higher transmittance when compared to our study. This can be explained by the Table 5.4.

The transmittance for sample 4 was measured by focusing the NIR light on the surface of the tissue. For this measurement the transmittance substantially increased when compared to the first three sample measurements. The focused light has narrower beam shape than the first case (1 mm distance between tissue and lens). Furthermore, focusing provides high directionality, thus more photons reached the photodiode without scattering which resulted in the increase of transmittance. Focusing the light inside the tissue rather than on the tissue surface increased the transmittance approximately five times at 7 mm tissue thickness ($T_{\text{first sample}}$= 13.5%, $T_{\text{fourth sample}}$= 61.86%). Similarly at 8 mm tissue thickness, focusing the NIR light on the tissue surface increased the NIR light transmission approximately five times. However, at 9 mm focusing the NIR light on the tissue surface hasn't provided a significant increase in the transmittance.

Rat tissue measurements showed a transmittance of 52% for 3 mm thick rat skin, approximately 40% for 5 mm thick thigh tissue with skin, and abdominal area where is rich in muscle has the transmittance of 25% at 10 mm tissue thickness. As expected, the transmittance was decreased as a result of increased tissue thickness. Transmittance through rat tissues is higher than pork tissues at the same tissue thicknesses. However, tissue types and structures were different between pork tissue samples and rat tissue samples. In order to compare the transmittance of pork tissue and rat tissue, samples should be taken from the same parts of the body to reduce the variability between transmittance results.

While determining the NIR light transmittance through tissue, temperature changes due to the light irradiation should be taken into account for safety reasons. The absorption of the NIR light by tissue induces a temperature elevation in the tissue. The temperature elevation is determined by the wavelength and beam shape of the light, pulsing parameters (i.e., pulse length, duty cycle, frequency), and power. Since we used an LED array as a light source, there are two sources of heat: the NIR light energy absorbed by the tissue and the conducted energy which is generated by the semiconductor junction inside the LED [49]. During the experiments, the duty cycle was 0.7%, the pulse width was 220 μs, and the frequency was 34 Hz. The peak of incident NIR light (875 nm) irradiance was 141.77 mW/cm^2 and the average irradiance was nearly 1 mW/cm^2.

The preliminary measurements on pork tissues with thermocouple demonstrated a temperature increase between 1.2 $^{\circ}C$ to 1.4 $^{\circ}C$. Ito et al., proposed a temperature increase of 0.3 ± 0.2 $^{\circ}C$ as a result of near infrared (789 nm) laser light irradiance [50]. Bozkurt et al., demonstrated a 0.5 $^{\circ}C$ temperature increase due to the NIR absorption and 9 $^{\circ}C$ temperature increase due to the conducted heat by LED.

The cell death as a result of temperature increase inside the cell occurs as the temperature exceeds 41 $^{\circ}$C [49].

According to the results the temperature elevation due to the NIR light is not at a level harmful to the tissue at the LED power levels tested in this project. Since in vivo experiments haven't done, the heat exchange mechanisms for reducing the temperature such as sweating, blood circulation, and exchange with air could not be accounted for.

5.3 Conclusions

Although in the NIR region the absorption and scattering properties of tissues are relatively low when compared to the rest of the light spectrum, the light transmittance through tissue is limited. The transmittance is decreased exponentially as the tissue thickness increased. The spot size of the incident light has a profound effect on the transmittance. The transmittance was approximately five times higher when the incident light was focused on the tissue surface for a tissue thickness of 9 mm.

The incident light properties such as wavelength, duty cycle, and power are important to transmit light most effectively through tissues. These properties determine the temperature elevation as well as a result of NIR light irradiation.

The results presented here allow for designing various transcutaneous telemetry systems with optimal light parameters.

5.4 Future Work

The sample size of the measurements can be increased to determine the transmittance more accurately. Including different tissue samples for investigation will give insights about the transmittance of those tissues. In our study, we used NIR LED array as a light source. The comparison of transmittance between LED, VCSEL and laser diode

for the same tissue thicknesses will provide useful information about their pros and cons for NIR light transmission through tissue. Furthermore, temperature elevations should be investigated along with these studies for determination of safety limits.

The results showed at 7 mm tissue thickness the photodiode current can go above 1 mA for a pulse width of 220 μs without causing too much of a temperature elevation. As the next step in this project, the current output of the photodiode can be connected to an implanted device in a rat and tested chronically for its efficacy.

REFERENCES

[1] M. Sahin and V. Pikov, "Wireless microstimulators for neural prosthetics," *Crit Rev Biomed Eng*. Vol. 39, pp. 63-77, 2011.

[2] B. C. Larson "An optical telemetry system for wireless transmission of biomedical signals across the skin," Doctoral thesis, Massachusetts Institute of Technology, Cambridge, MA, USA, 1999.

[3] J. H. Schulman, "The feasible FES system: battery powered BION stimulator," *Proceedings of the IEEE,* Vol. 96, pp. 1226-1239, 2008.

[4] P. Van der Zee, "Measurement and modelling of the optical properties of human tissue in the near infrared." Doctoral thesis, University of London, London, ,U.K., 1992.

[5] K. Inoue, K. Shiba, E. Shu, K. Koshiji, K. Tsukahara, T. Ohu-mi, et al., "Transcutaneous optical telemetry system-investigation on deviation characteristics," in *Engineering in Medicine and Biology Society, 1997. Proceedings of the 19th Annual International Conference of the IEEE*. Vol.5, pp. 2235-2237, 1997.

[6] T. D. Day. "Healing use light and color". Internet: http://www.healthcaredesignmagazine.com/article/healing-use-light-and-color, 2008, [March.28,2013].

[7] L. Goldman, S. Michaelson, R. Rockwell, D. Sliney, B. Tengroth, and M. Wolbarsht, "Optical radiation, with particular reference to lasers" in *Nonionazing Radiation Protection,* 2nd ed., Michael J. Suess, Deirde A. Benwell-Morison, Copenhagen, Denmark: WHO Regional Publications, 1989, pp. 49-84.

[8] W. T. Silfvast. "Fundamentals of photonics: Lasers″ Internet: http://spie.org/Documents/Publications/00%20STEP%20Module%2005.pdf, 2003, [March 28, 2013].

[9] H. Chung, T. Dai, S. K. Sharma, Y. Y. Huang, J. D. Carroll, and M. R. Hamblin, "The nuts and bolts of low-level laser (light) therapy," *Ann Biomed Eng*, vol. 40, pp. 516-533, 2012.

[10] J. T. Hashmi, Y. Y. Huang, B. Z. Osmani, S. K. Sharma, M. A. Naeser, and M. R. Hamblin, "Role of low-level laser therapy in neurorehabilitation," *PMR,*Vol. 2, pp. 292-305, 2010.

[11] H. T. Whelan, R. L. Smits, Jr., E. V. Buchman, N. T. Whelan, S. G. Turner, D. A. Margolis, et al., "Effect of NASA light-emitting diode irradiation on wound healing," *J Clin Laser Med Surg,* Vol. 19, pp. 305-314, 2001.

[12] J. S. Kana, G. Hutschenreiter, D. Haina, and W. Waidelich, "Effect of low-power density laser radiation on healing of open skin wounds in rats," *Arch Surg,* Vol. 116, pp. 293-296, 1981.

[13] G. Anneroth, G. Hall, H. Ryden, and L. Zetterqvist, "The effect of low-energy infra-red laser radiation on wound healing in rats," *Br J Oral Maxillofac Surg,* Vol. 26, pp. 12-17, 1988.

[14] H. T. B. Whelan, Ellen V.; Whelan, Noel T.; Turner, Scott G.; Cevenini, Vita; Stinson, Helen; Ignatius, Ron; Martin, Todd; Cwiklinski, Joan; Meyer, Glenn A.; Hodgson, Brian; Gould, Lisa; Kane, Mary; Chen, Gina; Caviness, James, "NASA light emitting diode medical applications from deep space to deep sea," *AIP Conference Proceedings,* vol. 552, pp. 35, 2001.

[15] A. Oron, U. Oron, J. Chen, A. Eilam, C. Zhang, M. Sadeh, *et al.*, "Low-level laser therapy applied transcranially to rats after induction of stroke significantly reduces long-term neurological deficits," *Stroke,* Vol. 37, pp. 2620-2624, 2006.

[16] Y. Lampl, J. A. Zivin, M. Fisher, R. Lew, L. Welin, B. Dahlof, et al., "Infrared laser therapy for ischemic stroke: a new treatment strategy: results of the NeuroThera Effectiveness and Safety Trial-1 (NEST-1)," *Stroke,* Vol. 38, pp. 1843-1849, 2007.

[17] Q. Wu, Y.-Y. Huang, S. Dhital, S. K. Sharma, A. C. H. Chen, M. J. Whalen, *et al.*, "Low level laser therapy for traumatic brain injury," *Proceedings of SPIE,* Vol. 7552, pp. 6-14, 2010.

[18] M. A. Naeser, A. Saltmarche, M. H. Krengel, M. R. Hamblin, and J. A. Knight, "Improved cognitive function after transcranial, light-emitting diode treatments in chronic, traumatic brain injury: two case reports," *Photomed Laser Surg,* Vol. 29, pp. 351-358, 2011.

[19] D. M. Ackermann, Jr., B. Smith, X. F. Wang, K. L. Kilgore, and P. H. Peckham, "Designing the optical interface of a transcutaneous optical telemetry link," *IEEE Trans Biomed Eng*, Vol. 55, pp. 1365-1373, 2008.

[20] K. Guillory, A. Misener, and A. Pungor, "Hybrid RF/IR transcutaneous telemetry for power and high-bandwidth data," *Conf Proc IEEE Eng Med Biol Soc*, Vol. 6, pp. 4338-4340, 2004.

[21] L. Tianyi, U. Bihr, S. M. Anis, and M. Ortmanns, "Optical transcutaneous link for low power, high data rate telemetry," in *Engineering in Medicine and Biology Society (EMBC), 2012 Annual International Conference of the IEEE*,, pp. 3535-3538, 2012

[22] A. Abdo, M. Sahin, D. S. Freedman, E. Cevik, P. S. Spuhler, and M. S. Unlu, "Floating light-activated microelectrical stimulators tested in the rat spinal cord," *J Neural Eng*, Vol. 8, pp. 056012, 2011.

[23] Y. Gil, N. Rotter, and S. Arnon, "Feasibility of retroreflective transdermal optical wireless communication," *Appl Opt*, Vol. 51, pp. 4232-4239, 2012.

[24] K. Goto, T. Nakagawa, O. Nakamura, and S. Kawata, "Near-infrared light transcutaneous telemetry system having an implantable transmitter driven by external laser irradiation," *Review of Scientific Instruments*,Vol. 72, pp. 3079-3085, 2001.

[25] E. Okamoto, Y. Yamamoto, Y. Inoue, T. Makino, and Y. Mitamura, "Development of a bidirectional transcutaneous optical data transmission system for artificial hearts allowing long-distance data communication with low electric power consumption," *J Artif Organs*, Vol. 8, pp. 149-153, 2005.

[26] J. Wells, P. Konrad, C. Kao, E. D. Jansen, and A. Mahadevan-Jansen, "Pulsed laser versus electrical energy for peripheral nerve stimulation," *J Neurosci Methods*, Vol. 163, pp. 326-337, 2007.

[27] J. Wells, M. Bendett, J. Webb, C. Richter, A. Izzo, E. D. Jansen, *et al.*, "Frontiers in optical stimulation of neural tissues: past, present, and future," *SPIE Proceedings*, Vol. 6854, pp. 68540B, 2008.

[28] J. Wells, C. Kao, K. Mariappan, J. Albea, E. D. Jansen, P. Konrad, *et al.*, "Optical stimulation of neural tissue in vivo," *Opt Lett*, Vol. 30, pp. 504-506, 2005.

[29] J. Wells, C. Kao, E. D. Jansen, P. Konrad, and A. Mahadevan-Jansen, "Application of infrared light for in vivo neural stimulation," *J Biomed Opt,* Vol. 10, pp. 064003, 2005.

[30] A. D. Izzo, J. T. Walsh, Jr., H. Ralph, J. Webb, M. Bendett, J. Wells, *et al.*, "Laser stimulation of auditory neurons: effect of shorter pulse duration and penetration depth," *Biophys J,* Vol. 94, pp. 3159-3166, 2008.

[31] J. Wells, C. Kao, P. Konrad, T. Milner, J. Kim, A. Mahadevan-Jansen, *et al.*, "Biophysical mechanisms of transient optical stimulation of peripheral nerve," *Biophys J,* Vol. 93, pp. 2567-2580, 2007.

[32] F. P. Bolin, L. E. Preuss, R. C. Taylor, and R. J. Ference, "Refractive index of some mammalian tissues using a fiber optic cladding method," *Appl Opt,* Vol. 28, pp. 2297-2303, 1989.

[33] G. Branco, "The development and evaluation of head probes for optical imaging of the infant head.," Doctoral thesis, University College London (UCL), U.K., 2007.

[34] N. Yavari, "Optical spectroscopy for tissue diagnostics and treatment control," Doctoral thesis, University of Bergen, Norway, 2006.

[35] C.-L. Tsai, J.-C. Chen, and W.-J. Wang, "Near-infrared absorption property of biological soft tissue constituents," *Journal of Medical and Biological Engineering,* Vol. 21, pp. 7-14, 2001.

[36] C. E. Elwell, "A practical users guide to near infrared spectroscopy." UCL Reprographics, London, U.K., 1995.

[37] T. Vo-Dinh, "Optical properties of tissue," in *Biomedical Photonics Handbook*., CRC Press, Boca Raton, FL:2003, pp. 33-83.

[38] A. Bashkatov, E. Genina, V. Kochubey, and V. Tuchin, "Optical properties of human skin, subcutaneous and mucous tissues in the wavelength range from 400 to 2000 nm," *Journal of Physics D: Applied Physics,*Vol. 38, pp.2543-2555, 2005.

[39] C. R. Simpson, M. Kohl, M. Essenpreis, and M. Cope, "Near-infrared optical properties of ex vivo human skin and subcutaneous tissues measured using the Monte Carlo inversion technique," *Physics in Medicine and Biology,* Vol. 43, pp. 2465-2478, 1999.

[40] I. C. o. N.-I. R. Protection, "ICNIRP statement on light-emitting diodes (leds) and laser diodes: implications for hazard assessment," *Health Physics*, Vol. 78, pp. 744-752, 2000.

[41] P. Optronics, "VCSEL Technology." Internet: http://www.princetonoptronics.com/technology/technology.php#VCSEL, [March 27, 2013]

[42] M. Hibbs-Brenner, K. Johnson, and M. Bendett, "VCSEL technology for medical diagnostics and therapeutics," *SPIE Biomedical Optics* , pp. 71800T-71800T-10, 2009

[43] H. Photonics, "Si photodiodes" in *Opto-Semiconducter Handbook,* Internet: http://www.hamamatsu.com/resources/pdf/ssd/e02_handbook_si_photodiode.pdf, [March 26, 2013]

[44] J. Fraden, "Light Detectors" in *Handbook of Modern Sensors: Physics, Designs, and Applications*, 3rd ed. Springer, San Diego, CA: 2003.

[45] "Enfis uno tag led array datasheet." Internet: http://www.enfis.com/files/Uno-Tag%20NIR.pdf, [March 28.2013]

[46] "MTD3010PM photodiode datasheet." Internet: http://www.marktechopto.com/products/datasheet/MTD3010PM, [March 28.2013]

[47] J. M. Conway, K. H. Norris, and C. Bodwell, "A new approach for the estimation of body composition: infrared interactance," *The American Journal of Clinical Nutrition*, Vol. 40, pp. 1123-1130, 1984.

[48] W. F. Cheong, S. A. Prahl, and A. J. Welch, "A review of the optical properties of biological tissues," *Quantum Electronics, IEEE Journal of*, Vol. 26, pp. 2166-2185, 1990.

[49] A. Bozkurt and B. Onaral, "Safety assessment of near infrared light emitting diodes for diffuse optical measurements," *Biomed Eng Online*, Vol. 3, pp. 9, 2004.

[50] Y. Ito, R. P. Kennan, E. Watanabe, and H. Koizumi, "Assessment of heating effects in skin during continuous wave near infrared spectroscopy," *J Biomed Opt*, Vol. 5, pp. 383-390, 2000.